(12) INTERNATIONAL APPLICATION PUBLISHED UNDER THE PATENT COOPERATION TREATY (PCT)

(19) World Intellectual Property Organization
International Bureau

(43) International Publication Date
22 May 2014 (22.05.2014)

WIPO | PCT

(10) International Publication Number
WO 2014/078423 A1

(51) International Patent Classification:
D01F 9/00 (2006.01) *H01M 4/1393* (2010.01)
B29C 47/88 (2006.01)

(21) International Application Number:
PCT/US2013/069906

(22) International Filing Date:
13 November 2013 (13.11.2013)

(25) Filing Language: English

(26) Publication Language: English

(30) Priority Data:
61/725,854 13 November 2012 (13.11.2012) US

(71) Applicant: **NDSU RESEARCH FOUNDATION** [US/US]; 1735 NDSU Research Park Drive Dept 4400, PO Box 6050, Fargo, North Dakota 58108-6050 (US).

(72) Inventors: **WU, Xiangfa**; 1735 NDSU Research Park Drive Dept 4400, PO Box 6050, Fargo, North Dakota 58108-6050 (US). **ZHOU, Zhengping**; 1735 NDSU Research Park Drive Dept 4400, PO Box 6050, Fargo, North Dakota 58108-6050 (US).

(74) Agents: **COLEMAN, Kyle S.** et al.; McKee, Voorhees & Sease, P.L.C., 801 Grand Avenue, Suite 3200, Des Moines, Iowa 50309-2721 (US).

(81) Designated States *(unless otherwise indicated, for every kind of national protection available)*: AE, AG, AL, AM, AO, AT, AU, AZ, BA, BB, BG, BH, BN, BR, BW, BY, BZ, CA, CH, CL, CN, CO, CR, CU, CZ, DE, DK, DM, DO, DZ, EC, EE, EG, ES, FI, GB, GD, GE, GH, GM, GT, HN, HR, HU, ID, IL, IN, IR, IS, JP, KE, KG, KN, KP, KR, KZ, LA, LC, LK, LR, LS, LT, LU, LY, MA, MD, ME, MG, MK, MN, MW, MX, MY, MZ, NA, NG, NI, NO, NZ, OM, PA, PE, PG, PH, PL, PT, QA, RO, RS, RU, RW, SA, SC, SD, SE, SG, SK, SL, SM, ST, SV, SY, TH, TJ, TM, TN, TR, TT, TZ, UA, UG, US, UZ, VC, VN, ZA, ZM, ZW.

(84) Designated States *(unless otherwise indicated, for every kind of regional protection available)*: ARIPO (BW, GH, GM, KE, LR, LS, MW, MZ, NA, RW, SD, SL, SZ, TZ, UG, ZM, ZW), Eurasian (AM, AZ, BY, KG, KZ, RU, TJ, TM), European (AL, AT, BE, BG, CH, CY, CZ, DE, DK, EE, ES, FI, FR, GB, GR, HR, HU, IE, IS, IT, LT, LU, LV, MC, MK, MT, NL, NO, PL, PT, RO, RS, SE, SI, SK, SM, TR), OAPI (BF, BJ, CF, CG, CI, CM, GA, GN, GQ, GW, KM, ML, MR, NE, SN, TD, TG).

Published:

— *with international search report (Art. 21(3))*

— *before the expiration of the time limit for amending the claims and to be republished in the event of receipt of amendments (Rule 48.2(h))*

(54) Title: NANOSTRUCTURED MATERIALS

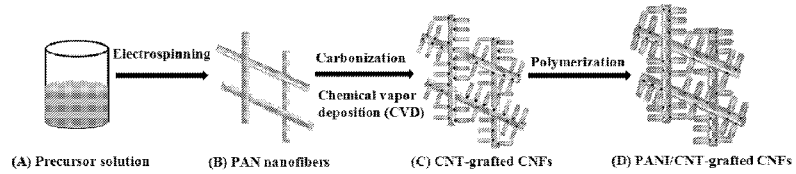

FIG. 14

(57) Abstract: The present invention describes materials created from various arrangements and uses of electrospun carbon nanofibers to create as hierarchical electrodes for supercapacitors. The morphology and microstructure of the electrodes were examined by electron microscopy, and the unique connectivity of the hybrid nanomaterials was responsible for the high specific capacitance and low intrinsic contact electric resistance of the hierarchical electrodes.

WO 2014/078423 A1

TITLE: NANOSTRUCTURED MATERIALS

CROSS-REFERENCE TO RELATED APPLICATIONS

This application claims priority under 35 U.S.C. §119 to provisional application Serial No. 61/725,854 filed November 13, 2012, herein incorporated by reference in its entirety.

GRANT REFERENCE

This invention was made with government support under Grant No. 43500 awarded by the Department of Energy. The government has certain rights in the invention.

BACKGROUND OF THE INVENTION

I. Field of the Invention

The present invention relates to the field of energy storage. More specifically, but not exclusively, the present invention relates to novel materials used in the creation of energy storage devices.

II. Description of the Prior Art

Energy consumption and production based on combustion of fossil fuels is deemed to have a severe future impact on the world's economy and ecology due to the decreasing availability of fossil fuels and global warming effect of greenhouse gas emissions. The future world will become more and more relying on sustainable and renewable energy resources such as solar, wind, and biomass based energies. In recent years, a rapid increase has been evidenced in renewable energy production from sunlight and wind, as well as the development of all-electric and plug-in hybrid electric vehicles (HEVs) with low carbon dioxide emission. Because of the fluctuation of solar and wind energies and the situation that we all expect to drive our cars with at least a few hours of autonomy, and love using convenient portable electronics and cordless tools for a longer duration, energy conversion and storage systems are essential to serve a large part of our lives. At the forefront of these are the electrical energy conversion and storage systems, such as rechargeable batteries, fuel cells, and electrochemical double-layer capacitors (EDLCs, supercapacitors, or ultracapacitors). Substantial improvement of their performance is highly desired in order to

match the increasingly eager demands of the future systems, ranging from mobile electronics and HEVs to large industrial equipment and electrical grid management, by developing new materials and devices and advancing our understanding of the electrochemical interface at the nanoscale.

Different from batteries and fuel cells which generate electrical energy by converting chemical energy into electrical energy via redox and reduction reactions at electrodes, supercapacitors store electrical energy by accumulating electrical charges in the double layers mainly by electrostatic force and can release the stored electrical energy without noticeable energy dissipation. The stored electrical energy in EDLCs is resulted from the separation of charged species across the electrode/electrolyte interfaces, and grows rapidly with increasing surface area of the electrodes. Figure 0A illustrates the porous electrodes of commercialized symmetric supercapacitors in the prior art, which are usually realized using porous carbon (e.g., coke) or activated carbon (AC). The specific surface area of activated porous carbon can reach the value as high as 3,000 m2/g. As a result, a very high capacitance value (up to 5,000 F) has been realized in commercial EDLCs made of AC electrodes.

Comparison of the charging/discharging behavior of EDLCs with rechargeable batteries is illustrated in the Ragone plot in Fig. 0B. One major disadvantage of current supercapacitors is their low energy density. Most of available commercial EDLCs have the energy density below 10 Wh/kg, whereas the lowest figure for rechargeable batteries is 35-40 Wh/kg, in the case of lead-acid ones, but the value up to 150 Wh/kg is also achievable for lithium-ion batteries. Nevertheless, EDLCs have much higher power density (typically in the range of 500-10,000 W/kg) than batteries (<1,000 W/kg). For this reason, EDLCs have been utilized in conjunction with batteries in power applications. Other advantages of EDLCs are related to their higher life cycle (>500,000 cycles), operation in a much wider range of temperature and higher charge/discharge rates (seconds to minutes). The unique electrochemical properties of EDLCs have made them highly attractive in today's green energy world where their ability to store energy quickly makes them particularly suitable for some specific applications, for instance the regenerative braking systems, whereas batteries have the difficulty due to their very low charge/discharge rates. However, substantial effort is still desired to make EDLCs with high enough energy density to be an attractive replacement for batteries in all-electric cars and plug-in hybrids, as EDLCs can

be quickly charged/discharged, exhibit temperature stability, and have very high efficiency in energy storage, among others.

The low energy density of EDLCs is resulted from the electrode structure and unique working mechanism of EDLCs as follows. (1) EDLCs store charges only at the electrode surfaces. The energy density of EDLCs is roughly proportional to the specific area of the electrode, however, it is much lower than that of batteries which store charges via ion intercalation (e.g., graphite, silicon, and LiCoO2 in Li-ion batteries), i.e., a process of volumetric storage of ions. (2) The potentials of EDLC electrodes swing between the low and high values during the charging/discharging process, while electrodes of batteries maintain nearly constant higher potentials during cycling. (3) Due to the ultrathin electrochemical double layer at electrode/electrolyte interface, the threshold potential of EDLCs is much lower than the output voltage of batteries. (4) The energy density of EDLCs is also limited by the depletion of ions in the electrolyte while rechargeable batteries (e.g., Li-ion batteries) maintain constant ion concentration in electrolyte.

Therefore, it is an object, feature, or advantage of the present invention to provide a novel interface self-healing technique for PMCs based on healant-loaded core-shell nanofibers.

It is another object, feature, or advantage of the present invention to provide a method of manufacturing the core-shell nanofibers that can be scaled to production quantities.

One or more of these and/or other objects, features or advantages of the present invention will become apparent from the specification and claims that follow.

SUMMARY OF THE INVENTION

The present invention provides several new, low-cost, flexible, porous, multifunctional electrodes made of hierarchally functionalized carbon nanofibers (CNFs) for use in supercapacitor-battery hybrids with high energy and power densities.

One exemplary embodiment provides a method for forming continuous multifunctional carbon nanofibers. The method includes, for example, using a precursor nanofiber solution and forming a nanofiber substrate from the solution. At least one nanotube is grown on the nanofiber substrate for forming a nanotube reinforced nanofiber

substrate. A nanostructured coating is deposited onto the nanotube reinforced nanofiber substrate.

Another embodiment provides a hierarchal nanotube grafted nanofiber structure. The structure includes, for example, a nanofiber substrate formed from a precursor nanofiber solution. At least one nanotube is grown on the nanofiber substrate. At least one nanostructured coating may be included on the nanotube nanofiber substrate.

Yet another embodiment provides a method for forming continuous multifunctional carbon nanofibers, for example, as a supercapacitor electrode. A backbone of nanofibers may be electrospun from a precursor nanofiber solution. By grafting at least one nanotube on the nanofiber backbone a nanotube reinforced nanofiber backbone may be formed. One or more conductive coatings may be deposited onto the nanotube reinforced nanofiber backbone for triggering a preferred pseudocapacitive effect during a charge/discharge process of a supercapacitor electrode.

BRIEF DESCRIPTION OF THE DRAWINGS

Illustrated embodiments of the present invention are described in detail below with reference to the attached drawing figures, which are incorporated by reference herein, and where:

Fig. 0A is a pictorial representation of charged electrochemical double-layer capacitor (EDLC) in accordance with an illustrative embodiment;

Fig. 0B is a pictorial representation of diagram for various electrical energy storage devices in accordance with an illustrative embodiment;

Fig. 1 is a pictorial representation of electron microscope micrographs in accordance with an illustrative embodiment;

Fig. 2 is a pictorial representation of a prototype supercapacitor made of hierarchical electrodes in accordance with an illustrative embodiment;

Fig. 3 is a pictorial representation of a cyclic voltammograms of the hierarchical electrodes at varied scanning rates in accordance with an illustrative embodiment;

Fig. 4 is a pictorial representation of potential-time discharge curves in accordance with an illustrative embodiment;

Fig. 5 is a pictorial representation of specific capacitance dependence on discharge current density in accordance with an illustrative embodiment;

Fig. 6 is a pictorial representation of a set of digital optical images in accordance with an illustrative embodiment;

Fig. 7 is a pictorial representation of TEM micrographs at low and high magnifications in accordance with an illustrative embodiment;

Fig. 8 is a pictorial representation of Raman spectra of CNFs (black) and G/CNFs (red) in accordance with an illustrative embodiment;

Fig. 9 is a pictorial representation of cyclic voltammograms of CNFs (black) and G/CNFs (red) samples in accordance with an illustrative embodiment;

Fig. 10 is a pictorial representation of cyclic voltammograms of G/CNFs samples in accordance with an illustrative embodiment;

Fig. 11 is a pictorial representation of charge-discharge curves of CNFs (black) and G/CNFs (red) in accordance with an illustrative embodiment

Fig. 12 is a pictorial representation of variation of specific capacitance of G/CNFs at varying current densities in accordance with an illustrative embodiment;

Fig. 13 is a pictorial representation of a cycling performance of G/CNF-based supercapacitors in accordance with an illustrative embodiment;

Fig. 14 is a pictorial representation of a schematic illustration of PANI nanowires growth on CNT-grafted CNF surfaces in accordance with an illustrative embodiment;

Fig. 15 is a pictorial representation of a set of SEM images in accordance with an illustrative embodiment;

Fig. 16 is a pictorial representation of FT-IR spectra of PANI/CNFs and PANI/CNT/CNFs in accordance with an illustrative embodiment;

Fig. 17 is a pictorial representation of cyclic voltammetry curves and Galvanostatic charge/discharge curves in accordance with an illustrative embodiment;

Fig. 18 is a pictorial representation of gravimetric capacitances and specific capacitance retention in accordance with an illustrative embodiment;

Figs. 19-20 are pictorial representations of a flow diagram and accompanying images for developing continuous multifunctional carbon nanofibers in accordance with an illustrative embodiment; and

Figs. 21-22 are pictorial representations of another flow diagram and accompanying images for developing continuous multifunctional carbon nanofibers in accordance with an illustrative embodiment.

DETAILED DESCRIPTION OF THE PREFERRED EMBODIMENTS

The disclosure comprises several new, low-cost, flexible, porous, multifunctional electrodes made of hierarchally functionalized carbon nanofibers (CNFs) for use in supercapacitor- battery hybrids with high energy and power densities. Supercapacitors and rechargeable batteries are two key types of devices for electrical energy conversion and storage that have founded extensive applications in portable electronics, power backup systems, hybrid electric vehicles (HEVs), etc. However, the cost, durability, charge/discharge rate, and energy and power density still limit their ever growing applications, especially in electric vehicles and electrical grid management.

Compared to existing supercapacitors in the market and reported in the literature, advantages of the novel electrodes released in this invention include follows. (1) Continuous CNFs produced via carbonization of low-cost as-electrospun polymer nanofibers carry high specific area and favorable electrical conductivity, which can be used as low-cost electrode material; grafting brush-like CNTs onto the CNFs can enhance in orders the specific surface area of the CNFs; the connectivity of CNTs via pinning covalently to the CNF substrate will effectively suppress the electrical contact resistance that commonly exists in electrodes made of discretely stacked nanomaterials. (2) Deposition of ultrathin layer of transition-metal oxides or conducting polymers on the surface of CNTs/CNFs will induce remarkable pseudocapacitive effect during cycling. (See, for example, Figs. 19-20 showing a flow diagram for developing continuous multifunctional carbon nanofibers (CNT-grafted CNFs coated with conducting polymer or transition metal oxides)) (3) Battery-supercapacitor hybrids made of these novel hierarchal CNF electrodes will substantially increase the specific capacitance as well as the energy and power densities. (4) The hierarchal CNFs are flexible and can be conveniently tailored to accommodate various electrode architectures for use in supercapacitor-battery hybrids.

The disclosure includes the following 6 exemplary types of nanostructured materials for use as supercapacitor electrodes:

Material 1: Continuous carbon nanofibers grafted with carbon nanotubes (CNTs).

Fabrication route: Electrospinning of polymer nanofibers, followed by controlled carbonization and chemical-vapor-deposition based CNT growth.

Material 2: Graphene-beaded continuous carbon nanofibers.

Fabrication route: Electrospinning of graphene/polymer nanofibers, followed by controlled carbonization.

Material 3: Ternary hierarchical CNT-grafted CNFs coated with conducting polymers.

Fabrication route: Electrospinning of polymer nanofibers, followed by controlled carbonization and in site polymerization in solution to coat conducting polymers.

Material 4: Graphene-beaded continuous carbon nanofibers coated with conducting polymers.

Fabrication route: Electrospinning of graphene/polymer nanofibers, followed by controlled carbonization and in site polymerization in solution to coat conducting polymers.

Material 5: Ternary hierarchical CNT-grafted CNFs coated with metal oxides.

Fabrication route: Electrospinning of polymer nanofibers, followed by controlled carbonization and in site electrical deposition of ultrathin metal oxide.

Material 6: Graphene-beaded continuous carbon nanofibers coated with metal oxides.

Fabrication route: Electrospinning of graphene/polymer nanofibers, followed by controlled carbonization and in site in site electrical deposition of ultrathin metal oxide.

These materials and the processes by which they are created will be described in additional detail in the remainder of this specification.

I. Continuous Carbon Nanofibers Grafted with Carbon Nanotubes

This section describes the fabrication and electrochemical properties of electrospun carbon nanofibers surface-grafted with vapor-grown carbon nanotubes (CNTs) as hierarchical electrodes for supercapacitors. The specific capacitance of the fabricated electrodes was measured up to 185 F/g at the low discharge current density of 625 mA/g; a

decrease of 38% was detected at the high discharge current density of 2.5 A/g. The morphology and microstructure of the electrodes were examined by electron microscopy, and the unique connectivity of the hybrid nanomaterials was responsible for the high specific capacitance and low intrinsic contact electric resistance of the hierarchical electrodes.

Due to fast consumption of fossil fuels and growing concern of climate change, today's society has become more and more relying on sustainable/renewable energy resources (e.g., solar, wind, geothermal, biomass energy, etc.), in which innovative materials and technologies for efficient storage and conversion of energy play a crucial role.[1] With the high specific power density, superior efficiency, fast charge/discharge rate, and long lifetime in harsh conditions, supercapacitors have been considered as a promising type of energy-storage devices supplemental to rechargeable batteries and hence have attracted extensive interests in recent years.[2-6] Several types of supercapacitors (including pseudo-supercapacitors) have been developed based on a variety of porous electrodes made of activated carbon, carbon nanotubes (CNTs), graphene, and carbon nanofibers (CNFs) surface-attached with metal (or metal oxide) nanoparticles or conductive polymers.[1-6] Among these, continuous CNFs (prepared via carbonization of polymer nanofiber precursors made by the technique of electrospinning[7-9]) have shown the great potential for the development of mechanically flexible/resilient, cost-effective, and property-tailorable electrodes for supercapacitors and rechargeable batteries.[10-14] When measured in KOH aqueous solution, the specific capacitance of the electrodes made of carbonized electrospun polyacrylonitrile (PAN) nanofibers (with diameters of 200- 400 nm) was 173 F/g at a low charge/discharge current density of 10 mA/g and 120 F/g at a high charge/discharge current density of 1,000 mA/g.10 The electrochemical performance of such electrodes can be further enhanced via improving the specific surface area of the CNFs through post-electrospinning treatment and/or via attaching metal (or metal oxide) nanoparticles on the CNFs to induce the pseudo-capacitive effect.[12-14] Herein, we report the fabrication of a type of hierarchical electrodes for solid-state supercapacitors with high specific surface area and superior intrinsic connectivity via grafting CNTs onto electrospun PAN-based CNFs.[15] The electrochemical performances and microstructures of the hierarchical electrodes were investigated.

During this study, the electrospinning technique[7-9] was utilized to fabricate continuous PAN nanofibers that were subsequently used as the precursor for making CNFs. The powders of PAN (MW = 150,000) and $Ni(AcAc)_2$ (purchased from the Sigma-Aldrich, Corp., St. Louis, MO) were dissolved in dimethylformamide (DMF) at the room temperature to prepare a solution with concentrations of PAN and $Ni(AcAc)_2$ being 13 wt.% and 5 wt.%, respectively. The solution was then filled into a 10 ml plastic syringe installed with a stainless steel needle (with the inner diameter: 0.48 mm). The electrospinning was carried out by applying a positive DC voltage of 18 kV (using an ES30P power supply purchased from the Gamma High Voltage Research, Inc., Ormond Beach, FL) between the spinneret and the collector (with the separation distance of 20 cm). The solution flow rate was set at 1.5 ml/h by a digital syringe pump (model number: KDS 200) purchased from the KD Scientific, Inc. (Holliston, MA).

The stabilization and carbonization of as-electrospun PAN/$Ni(AcAc)_a$ composite nanofibers (with diameters of 200-400 nm), as well as the growth of CNTs on the CNFs, were performed in a tubular reaction furnace purchased from the Atomate, Inc. (Santa Barbara, CA). The composite nanofibers were first stabilized in air to 215°C at a heating rate of 1°C/min followed by holding the temperature at 215°C for 1 h. Subsequently, the stabilized composite nanofibers were further carbonized in Ar to 500°C at a rate of 5°C/min. During this process, $Ni(AcAc)_2$ was decomposed into NiO. Thereafter, the carbonized nanofibers were treated at 500°C for 1 h in a mixture flow of H_2 and Ar (H_2/Ar = 1/2) to reduce NiO into elemental Ni, which would diffuse and aggregate into Ni nanoparticles on the nanofiber surface. The Ni nanoparticles served as catalyst for the growth of CNTs on the surface of CNFs. The sizes of Ni nanoparticles could be tuned via adjusting the temperature and duration of the process. After that, the samples were heated to 650°C at 5°C/min in an Ar flow and maintained at this temperature for 30 min; the Ar flow was then replaced with a mixture flow of Ar and C_2H_2 (Ar/C2H2 = 1) to grow CNTs. After reaction for 1 h, the C_2H_2 gas was turned off; and the furnace was cooled down to ambient temperature in Ar flow. Upon the above process, as- electrospun PAN/$Ni(AcAc)_2$ nanofibers were finally converted into CNFs surface-grafted with CNTs (Fig. 1). During the conversion of NiO into Ni nanoparticles, it was expected that the reducing agent of H_2 would result in the formation of H_2O, which would further react in situ with CNFs to generate tiny pores. This process would enhance the specific surface area of the CNFs.

Prototype solid-state supercapacitors were then fabricated by using the above CNT-grafted CNFs as electrodes. In this process, two CNT-grafted CNF mats with thickness of ~200 μm were used to sandwich a thin layer of polymer electrolyte; the electrolyte was a mixture of poly(vinyl alcohol) (PVA) and H3PO4 (10 wt.%),[16,17] as shown in Fig. 2. In addition, a mat of electrospun PAN nanofibers (with the diameters of 300-400 nm) was used as the separator to isolate the two hierarchical electrodes. Two pieces of copper foil were used as current collectors of the supercapacitors. The cyclic voltammetry and galvanostatic charging/discharging behavior were studied to evaluate the capacitive behavior and specific capacitance of the hierarchical electrodes, respectively, by using a supercapacitor tester (BT2000, Arbin Instruments, TX).

The morphology and microstructure of CNT-grafted CNFs were characterized with JEOL JSM-7600F/JEM-2100 scanning/transmission electron microscopes (SEM/TEM). The SEM micrographs (Figs. 1(a) & 1(b)) showed that CNTs were grafted on the surface of CNFs. In principle, primary factors that influence the specific capacitance of electric double-layer capacitors (EDLCs) are the specific surface area and electrical conductivity of the electrodes. The adopted method based on C_2H_2 as the carbon source and $Ni(AcAc)_2$ as the catalyst precursor to graft CNTs onto the surface of electrospun PAN-based CNFs can substantially increase the specific surface area and electrical conductivity of the hierarchical electrodes. In addition, at the reaction condition of 650°C in Ar, the formation of Ni nanoparticles on the CNF surface could be observed in the TEM micrograph (Fig. 1(c)). The sizes of Ni nanoparticles were in the range of 10-30 nm. The C_2H_2 gas was carried into the tubular reaction furnace and decomposed on the surface of Ni nanoparticles, where tubular nanostructure of multi-wall CNTs grew consequently on the electrospun CNFs.[15] The TEM image (Fig. 1(d)) shows the growth of CNTs with the outer diameters of 20-40 nm and the lengths of several microns. The diameter and length of the grafted CNTs could be tailored by adjusting the temperature, duration of the reaction, and carbon sources.[18] The Ni nanoparticles could be identified at the tip and middle locations of the CNTs due to different growth mechanisms.[18] The presence of Ni nanoparticles in CNFs could be advantageous to the performance of supercapacitors, because the Ni nanoparticles might carry the potential pseudo-capacitive effect.

Electrochemical properties of the hierarchical electrodes were characterized in the gel electrolyte of PVA with 10 wt. % H3PO4 by cyclic voltammetry. Fig. 3 shows the

current-voltage (CV) curves of the electrodes at several scanning rates (e.g., 5, 10, 30, and 50 mV/s). At the low scanning rates (e.g., 5 mV/s and 10 mV/s), the shapes of CV curves were nearly rectangular; i.e., the electrodes were stable in the gel electrolyte (See the inserted cyclic CV diagram at scanning rate of 10 mV/s in Fig. 3). In contrast, at the high scanning rates (e.g., 30 mV/s and 50 mV/s), the CV curves had been distorted with oblique angles. This indicated that high contact electric resistance existed between the electrodes and current collectors. The pseudo-capacitive behavior of Ni nanoparticles was not clearly identified from Fig. 3 (i.e., the Ni nanoparticles in this study exhibited the specific capacitance similar to that of carbon). In principle, the high specific surface area of the electrodes, the low volume fraction of Ni,[19] and the well-capsulation of Ni nanoparticles by the surrounding carbon might have shielded the pseudo-capacitive effect of Ni nanoparticles.

The typical potential-time discharge curves (chronopotentiograms) of the hierarchical electrodes tested in the PVA/H_3PO_4 gel electrolyte at 625 mA/g and 1875 mA/g, respectively, are plotted in Fig. 4. No significant IR drop was observed at the low discharge current of 625 mA/g, reflecting a low equivalent series resistance (ESR) of the electrodes. These results suggest that the unique connectivity of continuous CNFs surface-grafted with CNTs effectively improved the electric conductivity of the hierarchical electrodes; in contrast, the IR dropped noticeably with increase discharge current density.[20] The specific discharge capacitance (C) of the electrodes can be calculated using the relation:

$$C = 2 \times \frac{I \times \Delta t}{M \times \Delta V}$$

where I, Δt, and ΔV are the applied discharge current, time duration, and voltage change, respectively; M is the mass of the two electrodes. Fig. 5 shows the variation of the specific capacitance with respect to the discharge current density of the hierarchical electrodes in the PVA/H_3PO_4 gel electrolyte. The specific capacitance was up to 185 F/g at the discharge current density of 625 mA/g. Due to the high conductivity and large specific surface area of the hierarchical electrodes, the specific capacitance value of 114 F/g could be maintained even at the discharge current density as high as 2.5 A/g.

In summary, electrospun PAN-based CNFs surface-grafted with vapor-grown CNTs could be a type of hybrid nanomaterials to fabricate hierarchical (supercapacitor)

electrodes with high specific surface area and superior capacitive performance. Unlike discrete CNTs and/or CNTs coated with conductive polymers or attached with nanoparticles of metals (or metal oxides), the excellent connectivity of the developed nanofibrous materials could result in remarkable reduction of intrinsic contact electric resistance. Albeit the pseudo-capacitive effect of Ni nanoparticles was not noticeably identified in this study, such effect could be further explored through exposure of Ni nanoparticles to electrolyte via chemical or physical methods.

II. Graphene-Beaded Continuous Carbon Nanofibers

Fabrication and characterization of novel graphene-beaded nanofibrous carbon materials for use in supercapacitor electrodes is studied. The porous graphene-beaded carbon nanofiber (G/CNF) films were prepared by electrospinning polyacrylonitrile (PAN) / N,N-dimethylformamide (DMF) solution dispersed with graphene nanosheets, followed by carbonization at 800 °C. The morphology and chemical structure of the G/CNF films were characterized by means of scanning electron microscopy (SEM), transmission electron microscopy (TEM), and Raman spectroscopy. The electrochemical behavior of the synthesized G/CNF films as supercapacitor electrodes was characterized by cyclic voltammetry (CV) and galvanostatic charge/discharge in a 6 M KOH aqueous electrolyte. The results of electrochemical measurements revealed that the maximum specific capacitance of the porous G/CNF electrodes reached as high as 263.7 F/g at a discharge current density of 100 mA/g. In addition, the supercapacitor based on G/CNF electrodes exhibited an excellent cycling stability of electrical energy storage, with a retention percent of 86.9% after 2,000 cycles. The excellent electrochemical performance of G/CNFs was attributed to the unique structural configuration, high electrical conductivity and very large specific surface area of the graphene nanosheets.

a. Introduction

Supercapacitors [also called ultracapacitors or electrochemical double layer capacitors (EDLCs)] store and release electrical energy based on highly reversible electrolyte ions which form an electric double layer at the interface between the high-surface-area electrodes and electrolyte.[21,22] Compared to rechargeable batteries, supercapacitors carry higher specific power density (per unit mass) and energy/power efficiency, faster charge/discharge rate and longer lifetime even in harsh conditions. So far, supercapacitors, supplemental to batteries, have been finding rapidly expanding

applications in instant switches, portable electronics, backup power supply, regenerative braking system, motor starter, industrial power and energy management, and so on.[23-25] In principle, the specific capacitance of a supercapacitor relies on the specific surface area of the electrodes and the module voltage,[21,22] in which the former is determined by the porosity of the electrode material and the latter is governed by the dielectric property of the electrolyte. Besides, the energy/power efficiency and lifetime of a supercapacitor also depend on the electrical contact resistance within the electrodes and between the electrodes and the charge collectors.[26] Due to the low cost and high electrochemical stability, activated carbon has been extensively utilized in commercialized supercapacitors with the capacitance of a unit supercapacitor up to 5,000°F.[27,28] In addition, with the recent development of nanotechnology, carbon nanostructures such as carbon nanotubes (CNTs), carbon nanofibers (CNFs), graphene, etc. have been under intensive investigation as promising candidates of electrodes for use in supercapacitors with ultrahigh specific capacitance.[27-33]

Among various carbon nanostructures, graphene and continuous carbon nanofibers have also received increasing attention in recent years. Graphene is two dimensional (2D) graphitic material of single or multilayered graphitic sheet.[34,35] Graphene carries very large specific surface area (up to 3,100 m2/g of an individual graphene nanosheet), excellent electrical and thermal conductivities, and superior mechanical properties, which can also be conveniently fabricated and functionalized.[36-41] To date, exfoliated graphene nanosheets derived from natural graphite have been produced in large scale at low cost and without aid of extensive chemical oxidation.40 These graphene nanosheets with the average thickness of 3-5 nm typically consist of a few single-layer graphene sheets and have demonstrated as an attractive family of carbon nanomaterials for use in energy storage and onversion.[42,43] To date, a number of graphene-based nanomaterials have been reported for use as porous electrodes of supercapacitors with high specific capacitance.[44-48] The specific capacitance of these supercapacitors also depends upon the fabrication process of graphene; it is crucial to avoid the aggregation of graphene nanosheets in order to maintain the high specific surface area. Yet, due to the discrete nature of exfoliated graphene or graphitic nanoflakes, the graphene nanosheets stacked loosely in porous electrodes may lead to noticeable electrical contact resistance that may adversely decrease the energy/power efficiency of the supercapacitors.[46] New techniques are still desired to resolve the dilemma of achieving the

ultrahigh specific surface area and meanwhile maintaining the electrical connectivity between graphene nanosheets.

On the other hand, electrospinning technique as a low-cost, scalable, efficient top-down nanofabrication tool has been commonly utilized for producing continuous nanofibers of a large variety of polymers and polymer-derived carbon, metals, metal oxides, ceramics, etc.[49] Electrospinning provides versatile paths to produce low cost, porous nanofibrous electrodes for use in supercapacitors and rechargeable batteries.[50-52] Among these, continuous CNFs based on carbonization of as-electrospun polymer nanofibers are capable of providing sufficient electrical and thermal conductivities and very good electrical connectivity, and thus have raised particular interests in energy materials community. Several types of supercapacitors based on porous electrodes of electrospun CNFs have been successfully demonstrated with high specific capacitance, excellent cycling stability and low electrical resistance.[53-56] Yet, compared to CNTs and graphene, pure electrospun CNFs with the diameter of hundreds of nanometers normally carry relatively lower specific surface area, which limits the specific capacitance.

An exemplary method to synthesize and characterize an innovative porous electrode material for use in supercapacitors based on continuous graphene-beaded CNF (G/CNF) films is disclosed. The goal of the research was to comprehensively utilize the advantages of electrospun CNFs (e.g. continuity and electrical conductivity) and graphene (e.g. large specific surface area and high electrical conductivity) for use as a promising porous electrode material in supercapacitors. The porous G/CNF films were produced via electrospinning polyacrylonitrile (PAN)/N,N- dimethylformamide (DMF) solution dispersed with oxidized graphene nanosheets and consecutive carbonization; the morphology, chemical structure and electrochemical properties of the novel nanofibrous electrode material were characterized and compared with those based on pure electrospun CNFs (without graphene). The rest of this paper is formulated as follows. Section 2 delineates the experimental details to produce and characterize the novel porous G/CNF electrode material. Section 3 describes the results of structural and electrochemical measurements and potential mechanisms responsible for observed phenomena.

b. Experimental: Materials

Polyacrylonitrile (PAN, Mw = 150,000) powders and N,N-dimethylformamide (DMF, 99%) were purchased from Sigma-Aldrich Chemical Co. (St. Louis, MO, USA).

Commercial, as-grown, highly graphitic graphene nanosheets were supplied by XG Sciences, Inc. (Lansing, MI, USA). The graphene nanosheets containing oxygen (<1 wt%) had an average thickness of ~6-8 nm and a typical specific surface area of 120-150 m2/g. All the chemicals were used as received without further purification or modification.

c. Experimental: Preparation of Porous G/CNF Films

The precursor continuous G/PAN nanofibers were produced by electrospinning. The electrospinning solution consisting of graphene nanosheets and PAN in DMF was prepared by using the following route. PAN powder was first dissolved in DMF to prepare a 15 wt% PAN solution; well dispersed oxidized graphene nanosheets in DMF were then added into the PAN/DMF solution to achieve the concentrations of 10 wt% PAN and 1 wt% graphene nanosheets in DMF. The solution was prepared at a temperature of 80 °C with continuous stirring on a hotplate for 24 h. The as-prepared solution was placed into a 10-ml plastic syringe installed with a stainless spinneret, which was connected to a positive high voltage DC power supply purchased from the Gamma High Voltage Research, Inc. (Ormond Beach, FL). A laboratory-made aluminum rotary disk of the diameter of ~33 cm was connected to a grounded electrode as the nanofiber collector. The electrospinning process was performed in a high DC electrical field of 80 kV/m, which was maintained through applying a positive voltage 20 kV to a 25 cm gap between the spinneret and the grounded nanofiber collector. The flow rate of the electrospinning solution was fixed at 1.0 ml/h via a digital flow controller. After electrospinning, the nonwoven G/PAN nanofiber film was peeled off the aluminum foil and then dried at 100 °C in an oven for 6 h to remove the residual organic solvent prior to the stabilization treatment.

The stabilization and carbonization of the as-prepared G/PAN nanofiber films were performed in a tubular quartz furnace (Atomate, Inc., Santa Barbara, CA). The electrospun G/PAN nanofiber films were first heated up at a rate of 1 C/min and maintained at 215 °C for 1 h in air for the oxidative stabilization of PAN. The films were then carbonized as the temperature was increased from 215 to 800°C under Ar atmosphere at a rate of 5°C/min and annealed at 800°C for 30 min. Thereafter, the furnace was cooled down to 400°C in Ar and then kept at this temperature by introducing the air for 1 h for activation of the carbonized G/PAN nanofibers.

For the purpose of comparison, pure CNF films as control samples were also produced using the above procedure based on a 10 wt% PAN/DMF solution.

d. Experimental: Morphology and Structural Characterization

The surface morphology of both the G/CNF and CNF samples was analyzed by using a high-resolution field emission scanning electron microscope (FESEM, JEOL JSM-7600F). The microstructure of the G/CNF samples was further characterized by using a high-resolution transmission electron microscope (TEM, JEOL JEM-2100). The SEM samples of G/CNFs and CNFs were directly cut from the G/CNF and CNF films, respectively. The TEM samples were prepared by dispersing a small piece of G/CNFs into acetone and then depositing the G/CNFs on a TEM copper grid. The structural variation of G/CNF and CNF samples was identified by using a laser confocal Raman spectrometer (Nicolet NXR 9650 FT-Raman spectrometer, 632.8 nm).

e. Experimental: Electrochemical Measurements

Electrochemical characterization of the G/CNF samples was performed by using a symmetrical two-electrode cell setup. Such a setup is capable of providing accurate evaluation of the electrochemical performance of the porous nanofiber electrodes in supercapacitors.[57] The symmetrical two-electrode cell consisted of two pieces of 1.0 cm2 G/CNF films used as the two electrodes, two perforated nickel-copper sheets covered with the G/CNF films as the current collectors, and a 6 M KOH aqueous solution used as the electrolyte in a glass cell. The two current collectors were utilized to convey the electrical current from one electrode to the other. The cyclic voltammetry (CV) and galvanostatic charge/discharge curves were used to evaluate the electrochemical performance of the supercapacitor cells. These characteristic curves were recorded using a battery tester BT2000 (Arbin Instruments, TX, USA) and used for evaluating the capacitive behavior and calculating the specific capacitance of the porous G/CNF electrodes. In addition, the CV and galvanostatic charge/discharge measurements were performed in the potential range from 0 to 0.8 V with the scan rate from 5 to 100 mV s-1.

f. Results and Discussion: Morphology and Microstructures

Fig. 6(A) shows the micrograph of a typical electrospun G/CNF film. It can be observed that the G/CNF films based on carbonization of the precursor G/PAN nanofibers still maintain excellent flexibility and stretchable property. These G/CNFs with a unique connectivity between the graphene nanosheets would be suitable to be used as interconnects and electrodes in stretchable electronic devices. Figs. 6(B) and 6(C) show the typical FESEM micrographs of the pure CNFs and G/CNFs, respectively. The pure CNFs

prepared by electrospinning the precursor PAN nanofibers and consecutive carbonization carried relatively smooth surface morphology as shown in Fig. 6(B). The diameter of the CNFs is in the range of 300-400 nm. Figs. 6(C) and 6(D) show the low- and high-resolution FESEM micrographs of the G/CNFs, respectively. It can be clearly detected that the graphene nanosheets are closely jointed to the CNFs during electrospinning and afterward carbonization. These graphene nanosheets have a platelet shape with an average in-plane size of 1-5 microns and an average thickness of 6-8 nanometers. In general, graphene nanosheets can attain a large surface area and very high electrical conductivity, which may eliminate the need of conductive fillers and thus decrease the electrode thickness.

The TEM micrographs of G/CNF nanofibers are shown in Fig. 7(A) at a low magnification and Fig. 7(B) at a high magnification, respectively. As shown in Fig. 7(A), the graphene nanosheet is firmly connected at two ends with the CNF. The graphene nanosheets were electrospun and carbonized into CNFs, where the connection between the graphene nanosheets and the CNFs could be the strong covalent C-C bonds. Fig. 7(B) shows a typical linkage between a graphene nanosheet and the substrate/backbone CNF. At the edge of the graphene nanosheet, it can be clearly detected that a layer of graphene is out of the surface of the nanofiber.[58] Such unique morphology and structural properties are supposed to stabilize the three-dimensional (3D) structure of the electrodes during the charge-discharge cycle and to yield enhanced specific capacitance and cycling life of the supercapacitors.

Furthermore, the chemical microstructure of as-prepared CNFs was characterized by means of Raman spectroscopy in this study. Fig. 8 shows the comparison of the Raman spectra between CNFs (black) and G/CNFs (red) in the region of 800-2,200 cm-1. The Raman spectra of both the G/CNFs and pure CNFs exhibit two well-known bands of carbon at ~1,342 cm-1 and ~1,567 cm-1, i.e., the "D-band" and "G-band", respectively. The D-band is attributed to the disordered turbostratic structures or defects in the curved graphene nanosheets;[59] the G-band is related to the phonons propagating along the graphitic structures[60]. The intensity ratio of the D peak to the G peak, denoted by R=ID/IG, represents an amount of the ordered graphite crystallites in the CNFs. The R value of G/CNFs is 0.81, which is much lower than that of CNFs of 1.04. This difference indicates that the G/CNF films have more ordered graphite crystallites than pure CNF films due to

the addition of highly ordered graphitic nanosheets (~20 wt% in the final G/CNFs). In addition, addition of graphene nanosheets into PAN could potentially increase the transition ratio of disordered carbon into ordered graphite carbon in G/CNFs during carbonization process.

g. Results and Discussion: Electrochemical Properties

Figure 9 shows the typical CV curves of CNF and G/CNF electrodes with a scan rate of 5 mV/s and a potential window in the range of 0 to 0.8 V. The CV curve of G/CNF electrodes exhibits a nearly rectangle-shaped profile without obvious redox peaks, which is the characteristic of an ideal double-layer capacitor. In contrast, the CV curve of the control CNF electrodes becomes relatively distorted rectangular shape. Such a difference can be partially attributed to the improved internal electronic conductivity of the G/CNF electrodes due to the interplay of graphene nanosheets. Fig. 10 shows the CV curves of G/CNFs at varying potential scan rates of 5, 10, 30, 50, and 100 mV/s, which were measured within the potential window between 0 and 0.8 V in a 6 M KOH aqueous electrolyte, respectively. With the increase of potential scan rate, the CV profile still retains a nearly rectangular shape without obvious distortion even at the scan rate up to 100 mV/s.

To understand the electrochemical performance of the supercapacitors based on the novel porous nanofibrous electrodes, the galvanostatic charge/discharge of both the CNF and G/CNF films as electrodes was performed at varying constant current density, respectively. The average specific capacitance (C) of the supercapacitor is calculated as[53]

$$C = 2 \times \frac{I \times \Delta t}{M \times \Delta V}$$

where I is the constant charge/discharge current loaded (A), is the discharge time (s), is the potential difference (V) during discharge process, and M is the mass of G/CNFs or CNFs of a single electrode (gram). Figure 11 shows the representative charge/discharge curves of both the G/CNFs and pure CNFs at a constant current density of 500 mA/g. From these curves, the specific capacitance of G/CNF electrodes is calculated as 226.2 F/g, twice the capacitance of the pure CNF electrodes that is 114.6 F/g. It can also be observed that a voltage drop existed at the beginning of discharge, i.e., the IR drop that is attributed to the internal resistance of electrodes. It can be observed that the IR drop of G/CNF electrodes is much lower than that of the pure CNF electrodes. These results demonstrate that the unique interlaying graphene nanosheets could effectively suppress the internal electrical resistance of the electrodes. Variation of the specific capacitance of G/CNF electrodes as a function

with respect to the discharge current density in the range from 100 mA/g to 5 A/g is plotted in Fig. 12. In general, the instantaneous specific capacitance decreases with increasing discharge current density. The maximum instantaneous specific capacitance of G/CNF electrodes reaches as high as 263.7 F/g at a discharge current density of 100 mA/g. It is noteworthy that the specific capacitance of G/CNF electrodes can remain at a high value of 131.25 F/g even at a high discharge current density up to 2.5 A/g.

Electrochemical stability is one of the crucial factors in determining the potential applications of a supercapacitor,[55] which can be evaluated by the cycling life test. In this study, the constant current cycling test of the G/CNF based supercapacitors had been performed in a 6 M KOH aqueous solution over 2,000 cycles. The test was performed at a current rate of 2.5 A/g within the potential window of 0 to 0.8 V. Figure 13 shows the specific capacitance retention percent of G/CNFs as a function of the cycle number. The percent of capacitance retention 86.9% was maintained after 2,000 cycles. This result indicates the excellent electrochemical stability of the porous G/CNF electrodes during the cycling charge/discharge process. It can be concluded that graphene nanosheets within the G/CNF films acted as interconnectors to enhance the electrical conductivity and specific surface area of the electrodes for charge storage. Meanwhile, the CNFs also functioned as frameworks to link the graphene nanosheets and prevent the nanosheets from severe swelling and shrinking during cycling process.

h. Conclusions

Porous continuous G/CNFs have been successfully synthesized by electrospinning the solution of PAN/DMF dispersed with oxidized graphene nanosheets, followed by carbonization in a tubular quartz furnace. One of the major benefits is that the graphene nanosheets with very high specific surface area and excellent electrical properties can be beaded along with carbon nanofibers to achieve attractive heterogeneous carbon nanostructures. Such unique carbon nanostructures can significantly enhance the electrical connectivity of the graphene nanosheets and the effective specific surface area and electrical conductivity of the resulting G/CNFs. The electrochemical characterization performed in present study has demonstrated that the proof-of-concept supercapacitor based on the G/CNF electrodes carry superior electrochemical performance including very high specific capacitance, very low electrical resistance, and excellent cycling stability.

Thus, continuous porous G/CNF films can be a promising electrode material used for developing high-performance EDLCs in electrical energy storage and management.

III. Ternary Hierarchical CNT-grafted CNFs Coated with Conducting Polymers

Development of novel energy conversion and storage materials is one of the solutions to meet today's societal and environmental demands, which have become more and more relying on sustainable, clean and renewable energy resources. Among various energy conversion and storage devices, electrochemical capacitors (i.e., supercapacitors or ultracapacitors) are deemed as an efficient, competitive solution to the increasing need for high-power density energy storage devices.[61-63] Supercapacitor, often also called electrical double layer capacitors (EDLC), are common designed to bridge the gap between batteries and capacitors to form fast charging and discharging energy-storage devices of intermediate specific energy.[64] However, supercapacitors usually carry relatively low energy density compared to rechargeable batteries, which need to be further improved via developing new types of electrode materials.[65,66] PANI is one of the most studied materials as, since it not only has very high theoretical specific pseudocapacitance up to 750 F/g,[64,67] but also enhanced conductivity, sound environmental stability, and low-cost alternative to the relatively expensive metal oxides.[68] It has been reported that the pseudocapacitance of PANI gained from a reversible oxidation and reduction of the conjugated double bonds can reach the specific capacitance as high as 190 F/g.[69] Nevertheless, conductive polymers as monolithic electrodes may not meet the practical requirements since the pseudocapacitance of conductive polymers is limited by a number of factors, such as the redox switching, poor cyclic stability, and low life limit, among others.[70]

In order to suppress these drawbacks of conductive polymers for use in electrodes, herein we report a new type of ternary hierarchical core-shell-structured carbon nanofibers (CNFs) surface- grafted with carbon nanotubes (CNTs) and then coated with PANI nanowires. The synthesized ternary hierarchical core-shell-structured PANI/CNT-grafted CNF nanocomposites is expected to resolve the above two problems. In comparison to the CNT-grafted CNFs with low energy density, and PANI nanowires with poor electronic conductivity, this unique ternary hierarchical core-shell structure provides the critical features required for high-performance supercapacitors: 1) the intimate contacts between the PANI nanowires and the CNT-grafted CNF networks enable fast electron transport and effective current collection;[66,71] 2) CNT-grafted CNF 3D networks provide excellent

electronic conductivity which ensured high rate charge/discharge capability;[72,73] 3) the PANI nanowires coating on carbon surface with high surface areas, resulting in large specific capacitance and high energy density. Electrochemical results demonstrate that our synthesized PANI/CNT/CNF nanocomposite presents high energy/power density and excellent cycling and rate capability. This unique core-shell- structured composite is a promising candidate as an electrode material for supercapacitors.

The synthesis procedure of such ternary core-shell structure is based on two simple processes consisting of "top-down" electrospinning fabrication and "bottom-up" chemical vapor deposition and polymerization. As illustrated in Figure 14, we started with precursor solutions containing polyacrylonitrile (PAN) and nickel (II) acetylacetonate [$Ni(AcAc)_2$] dissolved in N,N- dimethylformamide (DMF) to electrospin into PAN nanofibers. These nanofibers were further underwent the carbonization and chemical vapor deposition (CVD) processes using ethylene (C2H4) as the carbon source to decompose to carbon species, which were grew into carbon nanotubes or nano-ribbons on the carbonized with the catalysis of Ni nanoparticles.[74] Subsequent polymerization of anilines, the percolating network of CNT-grafted CNFs provides a large, porous surface for the active sites of anilines, resulting in long ordered PANI nanowires grown on the surface of both CNTs and CNFs. Thereby, a ternary hierarchical core-shell structure with PANI grown on the CNT-grafted CNF surface was achieved.

Figure 15A, B, C and E show the typical scanning electron microscopy (SEM) images of the CNFs, CNT-grafted CNFs, PANI/CNFs and PANI/CNT/CNFs used in this study, respectively. The CNFs in the film have a smooth surface and uniform diameter in the range of 200 to 300 nm (Figure 15A). The entangled CNTs with the diameter of 20-30 nm were randomly grown on the surface of CNFs. The length of CNTs is about a few microns (Figure 15B). The diameter and length of the grown CNTs can be controlled by tuning the process and material parameters such as the catalyst, carbon sources, temperature, and duration of the reaction.[75] The CNT-grafted CNFs prepared by electrospinning and subsequent chemical vapor deposition CVD were highly porous with a rather rough surface layer compared to CNF surface. After in-situ polymerization based on aniline as the monomer and ammonium persulfate as catalyst, a layer of PANI nanowires was covered onto the surface of CNFs and CNT-grafted CNFs (Figure 15 C and E). High-magnification transmission electron microscopy (TEM) image of PANI/CNFs clearly

define that a long, ordered and need-like structured PANI nanowires is uniformly perpendicular on the CNF surface to form large-area arrays (Figure 15D).[76] It can be also observed that the PANI nanowires have an average diameters ranging from 50 to 80 nm. In addition, the length of the packed nanowires can be reached as long as 150 nm. The diameter and length of the PANI nanowires could be tailored by adjusting the concentration of aniline, temperature and duration of polymerization. Furthermore, PANI coated CNT-grafted CNFs also have proved that a hierarchical core-shell structure was generated via assembling nano-scaled CNTs with ultrathin leaf-like PANI film (Fig. 15F). Such process altered the surface morphology and provided a rougher surface, which guaranteed the high-performance of supercapacitors. Moreover, when used as porous electrodes in supercapacitors, the grafted CNTs also functioned as excellent current-delivery channel to suppress the electrical contact resistance of the electrodes due to high electrical conductivity and connectivity.

Figure 16 shows the typical FT-IR spectrum of the PANI/CNT-grafted CNFs and PANI/CNFs, respectively. The absorption peaks at 1564 cm-1 and 1465 cm-1 corresponds to the C–C stretching deformation mode of the quinoid (Q) and benzenoid (N) rings of PANI, respectively.[77] The peak at 3420 cm-1 is due to the N-H stretching vibration of PANI, while peaks at 1231 and 1294 are attributed to the C-N stretching vibration of an aromatic conjugation. The N-Q-N stretching band at 1087 is the characteristic band of PANI salt.[78] Thus, intensities of these peaks imply the formation of PANI layer on the surface of CNT-grafted CNFs. On the other hand, a characteristic band of CNT- grafted CNFs associated with C-C symmetric stretching was observed at 790 cm-1.

This unique ternary hierarchical core-shell-structure endows the hybrid materials as electrodes with excellent electrochemical performance. Figure 17A compares cyclic-voltammetry (CV) curves of (a) purified CNFs, (b) CNT-grafted CNFs, (c) PANI/CNFs, (d) PANI/CNT/CNFs electrodes at a potential scan rate of 5 mV/s in two-electrode cells using perforated nickel-copper sheets as the current collectors and 6 M KOH aqueous solution as the electrolyte. The nearly rectangular-shaped CV curves in a potential window of 0 V – 0.8 V of both (a) purified CNFs and (b) CNT-grafted CNFs-based electrodes show a typical capacitive behavior of supercapacitors. By comparison, at the same potential sweeping rate in a wider potential range of -0.8 V – 0.8 V, the CV plots of PANI/CNFs and PANI/CNT/CNFs-based electrodes display two pairs of current peaks, which are attributed

to the redox transition of PANI arrays of emeraldine form (conducting state)/ leucoemeraldine form (semiconducting state) and emeraldine-pernigraniline transformation, respectively.[79] In addition, the PANI/CNT/CNFs-based electrodes present a much better rate capability than the PANI/CNFs attributable to the improved internal electronic conductivity and high specific surface area of the nanocomposite derived from CNTs grafting and PANI coating.[71,74]

To further quantitatively determine the specific capacitances of these nanocomposites as electrodes, galvanostatic charge/discharge tests of symmetric device were performed at constant current density of 600 mA/g (Figure 17B). In comparison to purified CNFs, the CNT-grafted CNFs- based electrodes show an ideal linear shape due to excellent electronic conductivity and high specific surface area.[65] The unique structured electrodes exhibit high specific capacitance of 242.58 F/g and excellent coulombic efficiency of 98.01% (Table 1), which is much high than purified CNFs-based electrodes. However, the energy density of these electrodes is still not satisfactory. By contrast, the charge/discharge curves of PANI/CNFs and PANI/CNT/CNFs-based electrodes deviate from ideal linear shape, which derived from the faradic reversible pseudocapacitive characteristic of PANI nanowires.[80-81] The capacitance of PANI/CNFs and PANI/CNT/CNFs reaches as high as 295.04 F/g and 385.89 F/g, respectively, are all higher than that of previous electrodes. In particular, these hybrid composites display much high energy density and power density. For example, the energy density of PANI/CNT/CNFs can approach 137.3 Wh/kg at a power density of 973.0 W/kg. The results indicate that the presence of PANI nanowires does enhance not only the specific capacitance of PANI/CNF and PANI/CNT/CNF electrodes, but also the energy and power density. Meanwhile, the results also suggest that the core-shell-structured PANI nanowire arrays provide a shorten pathway for the ions and the charge transportation,[82] which resulting in a high-rate electrochemical capacitive performance.

Sample	Specific capacitance (F/g)		η %	Energy density	Power density
CNF	**143.2**	**130.8**	**91.34**	**11.62**	**470.02**
CNT/CNF	**247.5**	**242.58**	**98.01**	**21.56**	**485.1**
PANI/CNF	**316.27**	**295.04**	**93.29**	**104.9**	**968.3**
PANI/CNT/CNF	**386.86**	**385.89**	**99.75**	**137.3**	**973.0**

Table 1. List of electrochemical properties of all composites at current density of 600 mA/g.

Figure 18A compares the specific capacitance dependence on discharge current density (150 mA/g to 15A/g) of PANI/CNFs and PANI/CNT/CNFs-based electrodes. Clearly, the specific capacitance gradually decreases with increase of current densities for both PANI/CNFs and PANI/CNT/CNFs, which is a common feature for porous carbon electrodes.[83] However, PANI/CNT/CNF electrodes still retain a high specific capacitance of 220 F/g at a high current density of 15 A/g, which is about five times higher than that of PANI/CNF electrodes. The high rate capability further proves the importance of high internal electronic conductivity to enable fast electron transport and effective current collection. The excellent-performance electrodes consisting of core-shell structures were further analyzed the cycling behavior shown in Figure 18B. It can be observed that PANI/CNT/CNF-based electrodes show high specific capacitance retention of ≈90% after 2000 cycles of charge and discharge, which is much higher than that of PAN/CNFs.

In summary, we have synthesized a ternary hierarchical core-shell structure of PANI nanowires grown on CNT-grafted CNFs using a continuous, scalable approach, which is consisting of electrospinning, chemical vapor deposition, and in-situ polymerization technology. Benefiting from the 3D nano-architecture of CNT-grafted CNF, improved internal electronic conductivity, and the reversible pseudocapacitive characteristic and large specific surface area of PANI nanowires, PANI/CNT/CNF nanocomposite exhibits high specific capacitance, excellent energy and power density, and superior cycling stability. Based on these superior electrochemical performances, this unique ternary hierarchal core-shell-structured composite is a strong promising electrode for high- performance supercapacitors for energy storage and management.

a. Experimental: Preparation of CNT-grafted CNFs

The PAN/Ni(AcAc)$_2$ (ratio 5:2 by weight) composite nanofibers were fabricated by electrospinning. During the process, PAN and Ni(AcAc)$_2$ powders were dissolved in DMF to prepare a 10% wt. electrospinnable solution, which was then placed into a 10-ml plastic syringe installed with a stainless steel spinneret. Electrospinning was performed in a DC electric field of 90 kV/m, which was generated via applying a positive 18 kV voltage to a 20-cm gap between the spinneret and nanofiber collector.

The stabilization and carbonization of as-electrospun PAN/Ni(AcAc)$_2$ nanofibers were performed in a tubular furnace. The as-electrospun PAN/Ni(AcAc)$_2$ nanofibers were

first annealed at 215°C for 1h in air for oxidative stabilization, followed by heating up to 500°C at a rate of 5°C/min in Ar atmosphere. Subsequently, the CNFs were further annealed at 500°C in a mixed H_2 and Ar (H_2/Ar=1/2) flow for 1h to reduce Ni^{2+} to Ni atom. Ni atoms then aggregated onto CNF surface to form catalytic nanoparticles; these Ni nanoparticles functioned as catalyst to decompose hydrocarbon molecules into carbon atoms. Thereafter, the Ni/CNFs were heated up to 900°C at a rate of 5°C/min and annealed for 30 min in Ar flow for full carbonization. After that, the furnace was cooled down to 650°C in Ar and maintained at this temperature for 1h to grow CNTs by adopting a mixture flow of Ar and C_2H_4 (Ar/C_2H_4=1).

b. Experimental: Polymerization of Aniline on CNT-grafted CNF Mats

In-situ polymerization of aniline on CNT-grafted CNFs was prepared to follow the following route. A 0.03 M aniline solution in 200 mL 1 M sulfuric acid (H_2SO_4) was prepared first and cooled down to 0-5°C in a 500 mL flask. As-prepared CNT-grafted CNF mats (0.06 g dry weight) were then added to the aniline/sulfuric acid solution for 1h. Then, a 0.0075 M ammonium persulfate in 200 mL sulfuric acid solution was added in. The molar ratio of aniline/ ammonium persulfate was 4/1. The mixture solution was continuously stirred for 5 h polymerization at the same temperature of 0-5°C in an ice-bath[63]. During this period, the color of the solution was slowly changed to dark green. After polymerization, CNT-grafted CNF mat coated with PANI was filtered, and washed sequentially with deionized water and acetone. The product of PANI/CNT-grafted CNFs weighted 0.12 g after drying at a temperature of 70°C for 3 h. Exemplary flow charts for developing continuous multifunctional carbon nanofibers (i.e., Graphene-beaded CNFs coated with conducting polymer or transition metal oxides) are diagrammatically represented in Figs. 21-22.

c. Experimental: Electrochemical Measurements

The electrochemical performance of the supercapacitor cells was evaluated by cyclic voltammetry (CV) and galvanostatic charge/discharge in 6 M KOH electrolyte solution in the voltage range -0.8 V to 0.8 V. These data were obtained by using an Arbin BT-2000 testing system (Arbin Instruments, TX, USA) and used for evaluation of the capacitive behavior and calculation of the specific capacitance. The specific capacitance, C (F/g), was calculated according to

$$C = 2 \times \frac{I \times \Delta t}{M \times \Delta V}$$

where I is the constant charge/discharge current (A), Δt is the discharge time (s), ΔV is the potential difference (V) during discharge process, and M is the mass (grams) of composite in each electrode.

The present invention is not to be limited to the particular embodiments described herein. In particular, the present invention contemplates numerous variations in the type of ways in which embodiments of the invention may be applied in the creation of energy storage or other like devices. The foregoing description has been presented for purposes of illustration and description. It is not intended to be an exhaustive list or limit any of the disclosure to the precise forms disclosed. It is contemplated that other alternatives or exemplary aspects that are considered included in the disclosure. The description is merely examples of embodiments, processes or methods of the invention. It is understood that any other modifications, substitutions, and/or additions may be made, which are within the intended spirit and scope of the disclosure. For the foregoing, it can be seen that the disclosure accomplishes at least all of the intended objectives.

The previous detailed description is of a small number of embodiments for implementing the invention and is not intended to be limiting in scope. The following claims set forth a number of the embodiments of the invention disclosed with greater particularity.

REFERENCES

1. M. S. Whittingham, MRS Bulletin 33, 411 (2008)
2. http://en.wikipedia.org/wiki/Electric_double-layer_capacitor
3. P. Simon and Y. Gogotsi, Nature Mat. 7, 845 (2008).
4. X. Zhao, B. M. Sanchez, P. J. Dobson, and P. S. Grant, Nanoscale 3, 839 (2011).
5. E. Frackowiak, Phys. Chem. Chem. Phys. 9, 1774 (2007).
6. V. V. N. Obreja, Physica E 40, 2596 (2008).
7. D. H. Reneker and I. Chun, Nanotechnology 7, 216 (1996).
8. D. H. Reneker, A. L. Yarin, E. Zussman, and H. Xu, Adv. Appl. Mech. 41, 43 (2006).
9. D. H. Reneker and A. L. Yarin, Polymer 49, 2387 (2008).
10. C. Kim and K. S. Yang, App. Phys. Lett. 83, 1216 (2003).
11. J. J. Miao, M. Miyauchi, T. J. Simmons, J. S. Dordick, and R. J. Lindardt, J. Nanosci. Nanotech. 10, 5507 (2010).

12. X. W. Zhang, L. W. Ji, O. Toprakci, Y. Z. Liang, and M. Alcoutlabi, Polym. Rev. 51, 239 (2011).

13. L. W. Ji and X. W. Zhang, Carbon 47, 3219 (2009).

14. L. W. Ji, Z. Lin, A. J. Medford, and X. W. Zhang, Carbon 47, 3346 (2009).

15. C. L. Lai, Q. H. Guo, X. F. Wu, D. H. Reneker, and H. Q. Hou, Nanotechnology 19, 195303 (2008).

16. M. Kaempgen, C. K. Chan, J. Ma, Y. Cui, and G. Gruner, Nano Lett. 9, 1872 (2009).

17. J. H. Sung, S. J. Kim, S. H. Jeong, E. H. Kim, and K. H. Lee, J. Power Sources 162, 1467 (2006).

18. J. Ziebro, I. Lukasiewicz, E. Borowiak-Palen, and B. Michalkiewicz, Nanotechnology 21, 145308 (2010).

19. V. Srinivasan and J. W. Weidner, J. Electrochem. Soc. 144, 8 (1997).

20. Q. Guo, X. Zhou, X. Li, S. Chen, A. Seema, A. Greiner, and H. Hou, J. Mater. Chem. 19, 2810 (2009).

21. M.Winter and R. J. Bridd, Chem. Rev., 2004, 104, 4245.

22. R. Kötz and M. Carlen, Electrochim Acta, 2000, 45, 2483.

23. J. R. Miller and P. Simon, Science, 2008, 321, 651.

24. J. R. Miller and A. F. Burke, Electrochem Soc. Interface, 2008, 17, 53.

25. B. Andrew, J Power Sources, 2000, 91, 37.

26. X.-F. Wu, Z. P. Zhou, and W. M. Zhou, Appl. Phys. Lett., 2012; 100, 193115.

27. E. Frackowiak and F. Béguin, Carbon, 2001, 39, 937.

28. A. G. Pandolfo and A. F. Hollendamp, J. Power Source, 2006, 157, 11.

29. V. V. N. Obreja, Physica E: Low-dimensional. Sys. Nanostruct., 2008, 40, 2596.

30. L. L. Zhang and X. S. Zhao, Chem. Sov. Rev., 2009, 38, 2520.

31. M. Inagaki, H. Konno, and O. Tanaike, J. Power Sources, 2010, 195, 7880.

32. P. Simon and Y. Gogotsi, Nature Mater., 2008, 7, 845.

33. D. S. Su and R. Schlögl, ChemSusChem, 2010, 3, 136.

34. M. I. Katsnelson, Mater. Today, 2007, 10, 20.

35. K. S. Novoselov, Rev. Modern Phys. 2011, 83, 837.

36. A. A. Balandin, S. Ghosh, W. Z. Bao, I. Calizo, D. Teweldebrhan, F. Miao, and C. N. Lau, Nano Lett., 2008, 8, 902.

37. A. H. C. Neto, F. Guinea, N. M. R. Peres, K. S. Novoselov, and A. K. Geim, Rev. Modern Phys., 2009, 81, 109.

38. C. Lee, X. D. Wei, J. W. Kysar, and J. Hone, Science, 2008, 321, 385.

39. K. P. Loh, Q. L. Bao, P. K. Ang, and J. X. Yang, J. Mater. Chem., 2010, 20, 2277.

40. L. T. Drzal and H. Fukushima, U.S. Patent, 2004, 20040127621.

41. W. B. Wan, Z. B. Zhao, Y. R. Fan, H. Hu, Q. Zhou, and J. S. Qiu, Prog. Chem., 2011, 23, 1883.

42. D. A. C. Brownson, D. K. Kampouris, and C. E. Banks, J. Power Sources, 2011, 196, 4873.

43. S. Biswas and L. T. Drzal, ACS Appl. Mater. Interfaces, 2010, 2, 2293.

44. M. D. Stoller, S. J. Park, Y. W. Zhu, J. An, and R. S. Ruoff, Nano Lett. 2008, 8, 3498.

45. C. G. Liu, Z. N. Yu, D. Neff, A. Zhamu, and B. Z. Jang, Nano Lett. 2010, 10, 4863.

46. Q. Wu, Y. X. Xu, Z. Y. Yao, A. R. Liu, and G. Q. Shi, ACS Nano, 2010; 4, 1963.

47. K. Zhang, L. L. Zhang, X. S. Zhao, and J. S. Wu, Chem. Mater., 2010, 22, 1392.

48. Y. W. Zhu, S. Murali, M. D. Stoller, K. J. Ganesh, W. W. Cai, P. J. Ferreira, A. Pirkle, R. M. Wallace, K. A. Cychosz, M. Thommes, D. Su, E. A. Stach, and R. S. Ruoff, Science, 2011, 332,1537.

49. D. H. Reneker, A. L. Yarin, E. Zussman, and H. Xu, Adv. Appl. Mech., 2006, 41, 43.

50. J. J. Miao, M. Miyauchi, T. J. Simmons, J. S. Dordick, and R. J. Linhardt, J. Nanoscience Nanotechnology, 2010, 10, 5507.

51. Z. X. Dong, S. J. Kennedy, and Y. Q. Wu, J. Power Sources, 2011, 196, 4886

52. X. W. Zhang, L. W. Ji, O. Toprakci, Y. Z. Liang, and M. Alcoutlabi, Polym. Rev., 2011, 51, 239.

53. C. Kim and K. S. Yang, Appl. Phys. Lett., 2003, 83, 1216.

54. Q. H. Guo, X. P. Zhou, X. Y. Li, S. L. Chen, A. Seema, A. Greiner, and H. Q. Hou, J. Mater. Chem., 2008, 19, 2810.

55. Y. Hou, Y. W. Cheng, T. Hobson, and J. Liu, Nano Lett., 2010, 10, 2727.

56. Z. P. Zhou, X. F. Wu, and H. Fong, Appl. Phys. Lett. 2012, 100, 023115.

57. V. Khomenko, E. Frackowiak, and F. Beguin, Electrochim Acta, 2005, 50, 2499.

58. C. L. Lai, Q. H. Guo, X. F. Wu, D. H. Reneker, and H. Q. Hou, Nanotechnology, 2008, 19, 195303.

59. Z. P. Zhou, K. M. Liu, C. L. Lai, L. F. Zhang, J. H. Li, H. Q. Hou, D. H. Reneker, H. Fong, Polymer, 2010, 51, 2360.

60. V. Barranco, M. A. Lillo-Rodenas, A. Linares-Solano, A. Oya, F. Pico, J. Ibañez, F. Agullo-Ruedav, J. M. Amarilla, and J. M. Rojo, J. Phys. Chem. C, 2010, 114, 10302.

61. J. R. Miller, P. Simon, Science 2008, 321, 651.

62. J. Chmiola, G. Yushin, Y. Gogotsi, C. Portet, P. Simon, P. L. Taberna, Science 2006, 313, 1760.

63. P. Simon, Y. Gogotsi, Nat. Mater. 2008, 7, 845.

64. G. A. Snooka, P. Kaob, A. S. Best, J. Power Sources 2011, 196, 1.

65. Q. Qu, Y. Zhu, X. Gao, Y. Wu, Adv. Energy. Mater., DOI: 10.1002/aenm.201200088.

66. X. Wang, G. Li, Z. Chen, V. Augustyn, X. Ma, G. Wang, B. Dunn, Y. Lu. Adv. Energy. Mater. 2011, 1, 1089.

67. K. Lota, V. Khomenko, E. Frackowiak, J. Phys. Chem. Solids 2004, 65, 295.

68. X. Zhao, B. M. Sánchez, P. J. Dobson, P. S. Grant, Nanoscale 2011, 3, 839.

69. Y. K. Zhou, B. L. He, W. J. Zhou, J. Huang, X. H. Li, B. Wu, and H. L. Li, Electrochim. Acta 2004, 49, 257.

70. X. Zhao, B. M. Sanchez, P. J. Dobson, and P. S. Grant, Nanoscale 2011, 3, 839.

71. X. F. Wu, Z. P. Zhou, W. M. Zhou, Appl. Phys. Lett. 2012, 100, 193115.

72. Z. Chen, J. Wen, C. Yan, L. Rice, H. Sohn, M. Shen, M. Cai, B. Dunn, Y. Lu, Adv. Energy. Mater. 2011, 1, 551.

73. C. Portert, G. Yushi, Y. Gogotsi, J. Electrochem. Soc. 2008, 155, A531.

74. Z. P. Zhou, X. F. Wu, H. Fong, Appl. Phys. Lett. 2012, 100, 023115.

75. C. L. Lai, Q. H. Guo, X. F. Wu, D. H. Reneker, H.Q. Hou, Nanotech. 2008, 19, 1.

76. S. J. He, X. W. Hu, S. L. Chen, H. Hu, M. Hanif, H. Q. Hou, J. Mater. Chem. 2012, 22, 5114.

77. Q. W. Tang, J. H. Wu, X. M. Sun, Q. H. Li, J. M. Lin, Langmuir 2009, 25, 5253.

78. D. S. Yuan, T. X. Zhou, S. L. Zhou, W. J. Zou, S. S. Mo, N. N. Xia, Electrochem. Commun. 2011, 13, 242.

79. C. C. Hu, J. Y. Lin, Electrochin. Acta 2002, 47, 4055.

80. S. Biswas, L. T. Drzal, Chem. Mater. 2010, 22, 5667.

81. S. Li, Y. Luo, Wei Lv, Wanjing Yu, Sida Wu, Pengxiang Hou, Quanhong Yang, Qingbo Meng, Chang Liu, H.-M. Cheng, Adv. Energy. Mater. 2011, 1, 486.

82. Q. H. Guo, X. P. Zhou, X. Y. Li, S. L. Chen, A. Seema, A. Greiner, H. Q. Hou, J. Mater. Chem. 2008, 19, 2810.

83. C. Meng, C. Liu, L. Chen, C. Hu, S. Fan. Nano Lett. 2010, 10, 4025.

What is claimed is:

1. A method for forming continuous multifunctional carbon nanofibers comprising:

providing a precursor nanofiber solution;

forming a nanofiber substrate from said solution;

growing at least one nanotube on the nanofiber substrate forming a nanotube reinforced nanofiber substrate; and

depositing a nanostructured coating onto said nanotube reinforced nanofiber substrate.

2. The method of claim 1 further comprising:

electrospinning said nanofiber substrate from said precursor nanofiber solution.

3. The method of claim 1 further comprising:

selecting said precursor nanofiber solution from at least one of:

a. a blended metal salt polymer;

b. a blended graphene nanosheet polymer.

4. The method of claim 1 further comprising:

growing the nanotube by chemical vapor deposition.

5. The method of claim 1 further comprising:

selecting said nanostructured coating from one of:

a. a nanostructured conducting polymer;

b. a transition metal oxide.

6. The method of claim 5 further comprising:

depositing said nanostructured conducting polymer by in situ polymerization.

7. The method of claim 5 further comprising:

depositing said transition metal oxide by controlled pyrosis.

8. A hierarchical nanotube grafted nanofiber structure comprising:
a nanofiber substrate formed from a precursor nanofiber solution;
at least one nanotube grown on the nanofiber substrate; and
at least one nanostructured coating on said nanotube nanofiber substrate.

9. The structure of claim 8 wherein said nanofiber substrate comprises an electrospun fiber.

10. The structure of claim 8 wherein the precursor nanofiber solution comprises at least one of:

a. a blended metal salt polymer;
b. a blended graphing nanosheet polymer.

11. The structure of claim 8 further comprising:
a chemical growth catalyst for the at least one nanotube.

12. The structure of claim 8 wherein the nanostructured coating comprises at least one of:

a. a nanostructured conducting polymer;
b. a transition metal oxide.

13. The structure of claim 8 further comprising at least one electrode for receiving and discharging electricity stored in the nanotube nanofiber substrate.

14. A method for forming continuous multifunctional carbon nanofibers comprising:
electrospinning a nanofiber backbone from a precursor nanofiber solution;
grafting at least one nanotube on the nanofiber backbone;
forming a nanotube reinforced nanofiber backbone; and
depositing a conductive coating onto said nanotube reinforced nanofiber backbone.

15. The method of claim 14 further comprising:
selecting said precursor nanofiber solution from at least one of:

a. a blended metal salt polymer;

b. a blended graphene nanosheet polymer.

16. The method of claim 14 wherein the nanotube reinforced nanofiber backbone comprises carbon nanotube-grafted carbon nanofibers.

17. The method of claim 14 wherein the nanotube reinforced nanofiber backbone comprises graphene-beaded carbon nanofibers.

18. The method of claim 14 wherein the conductive coating comprises one or more nanostructured conducting polymers deposited by polymerization.

19. The method of claim 14 wherein the conductive coating comprises one or more transition metal oxides deposited by controlled pyrosis.

20. The method of claim 14 further comprising:
forming a supercapacitor electrode with the nanotube reinforced nanofiber backbone.

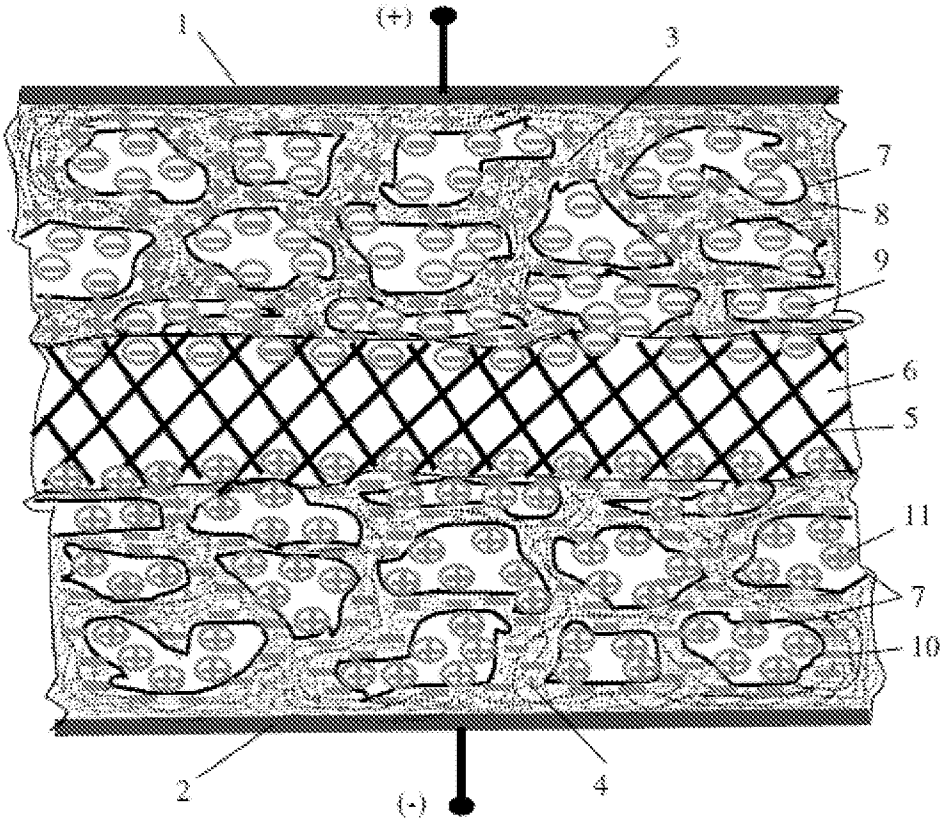

FIG. 0A

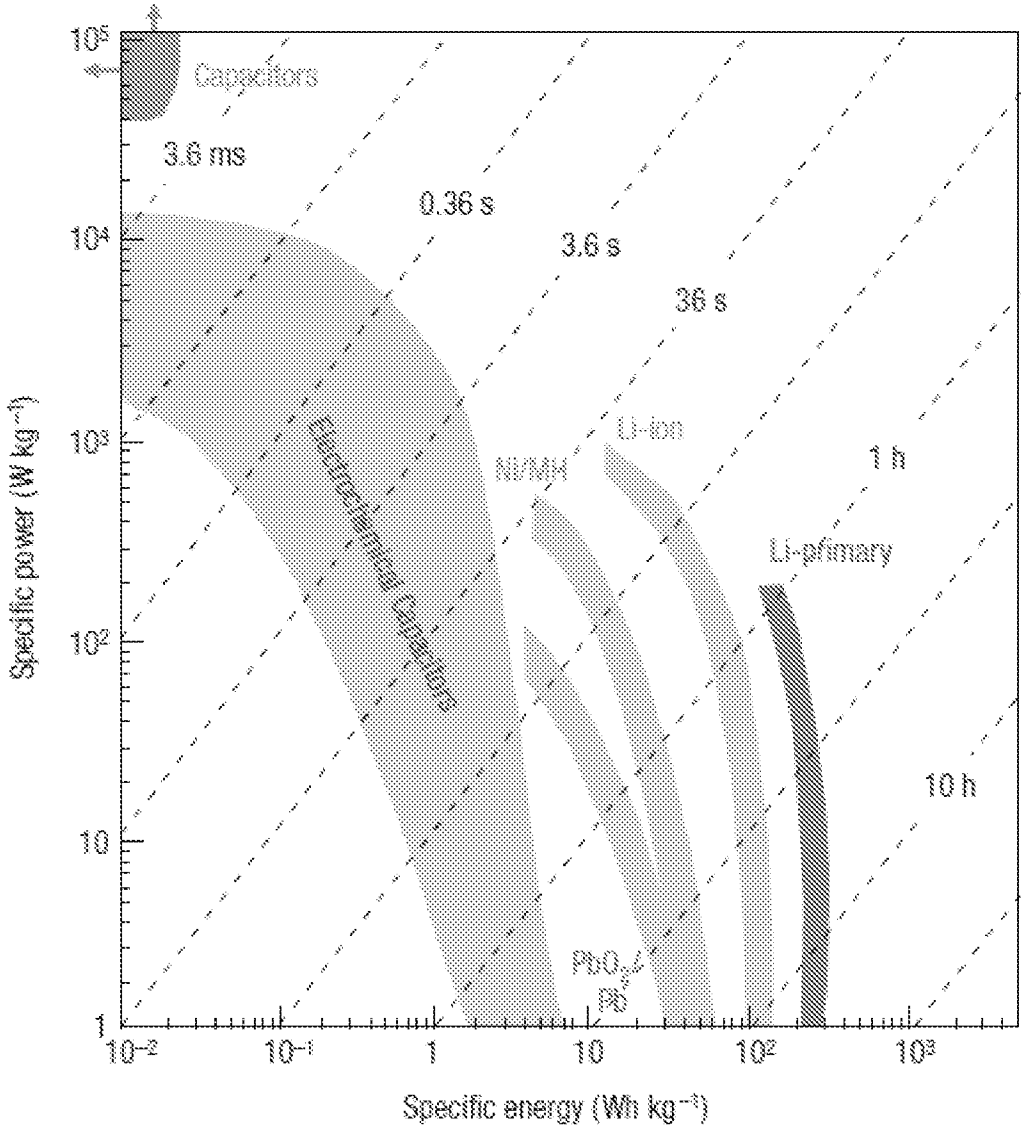
Capacitors
3.6 ms
0.36 s
3.6 s
36 s
1 h
10 h
Electrochemical Capacitors
Ni/MH
Li-ion
Li-primary
PbO2
Pb
Specific power (W kg−1)
Specific energy (Wh kg−1)
10−2
10−1
1
10
10²
10³
10⁴
10⁵

FIG. 0B

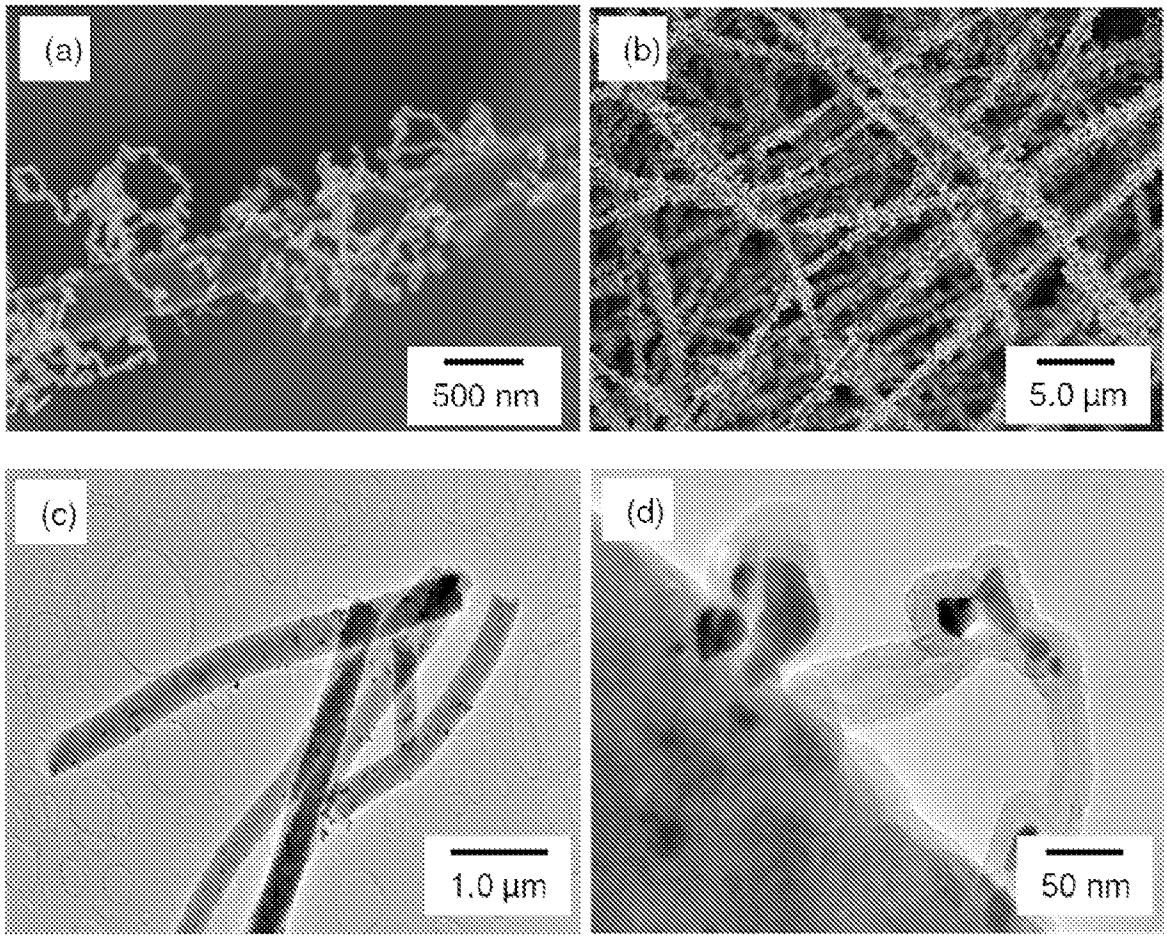

FIG. 1

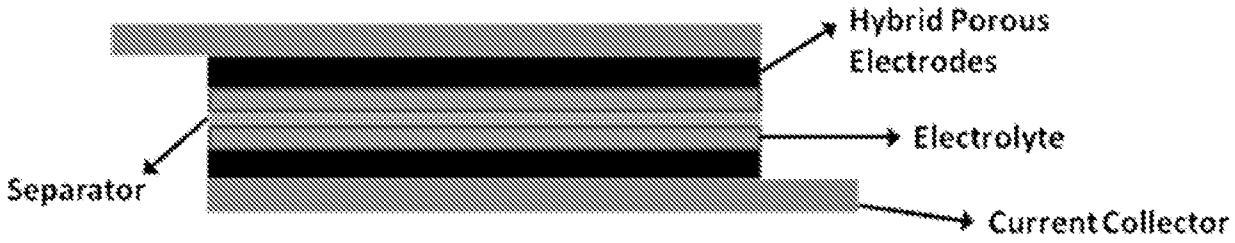
Hybrid Porous
Electrodes
Electrolyte
Separator
Current Collector

FIG. 2

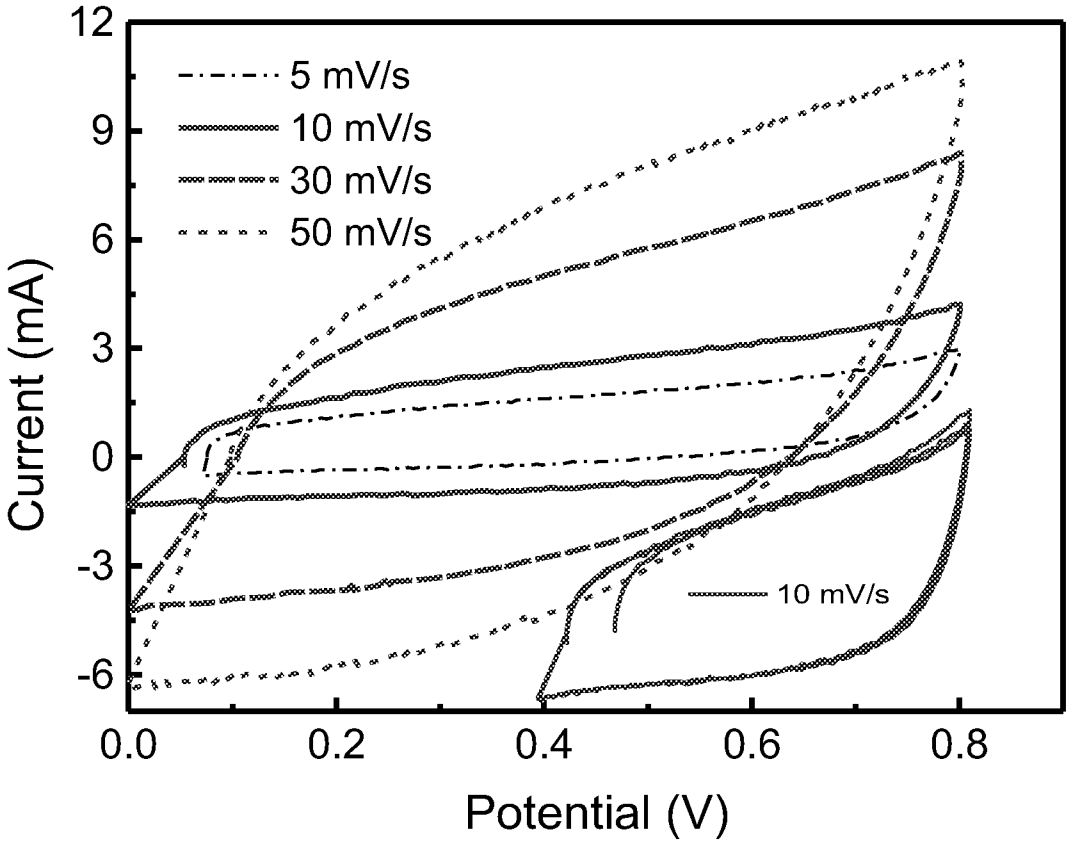
12
9
6
3
0
-3
-6
Current (mA)
0.0
0.2
0.4
0.6
0.8
Potential (V)
5 mV/s
10 mV/s
30 mV/s
50 mV/s
10 mV/s

FIG. 3

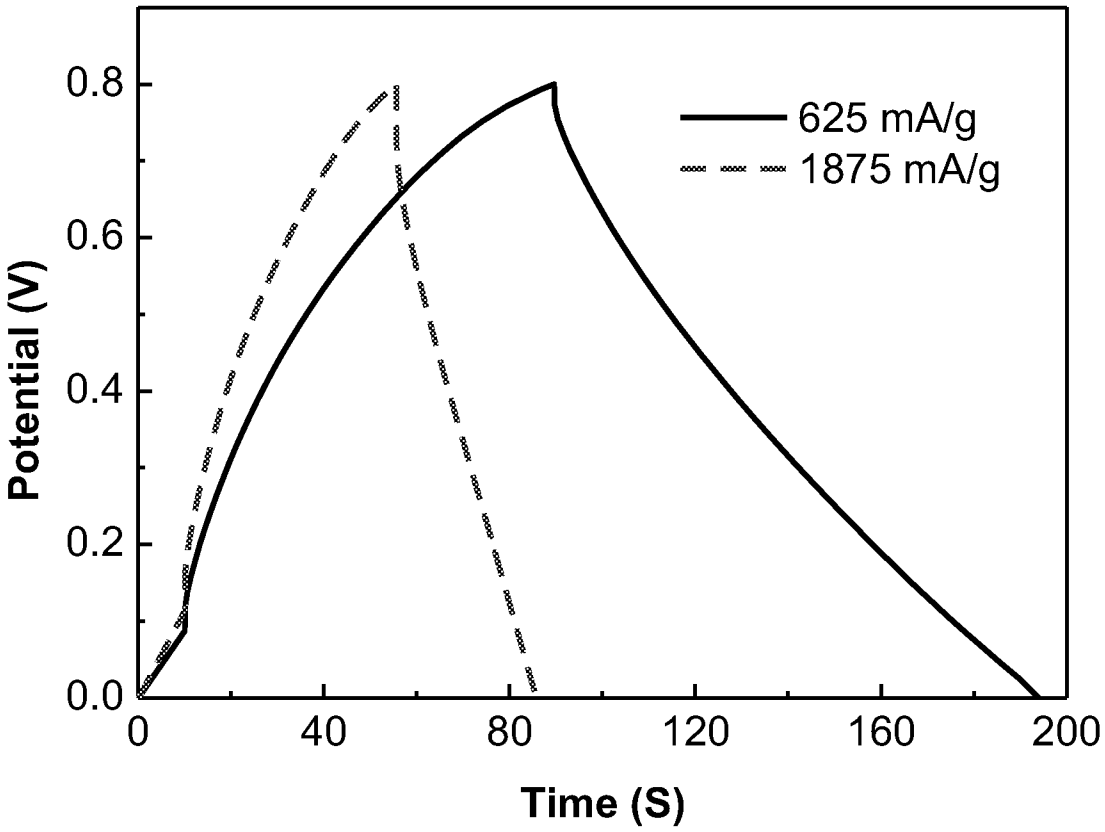
0.8
0.6
0.4
0.2
0.0
Potential (V)
0
40
80
120
160
200
Time (S)
625 mA/g
1875 mA/g

FIG. 4

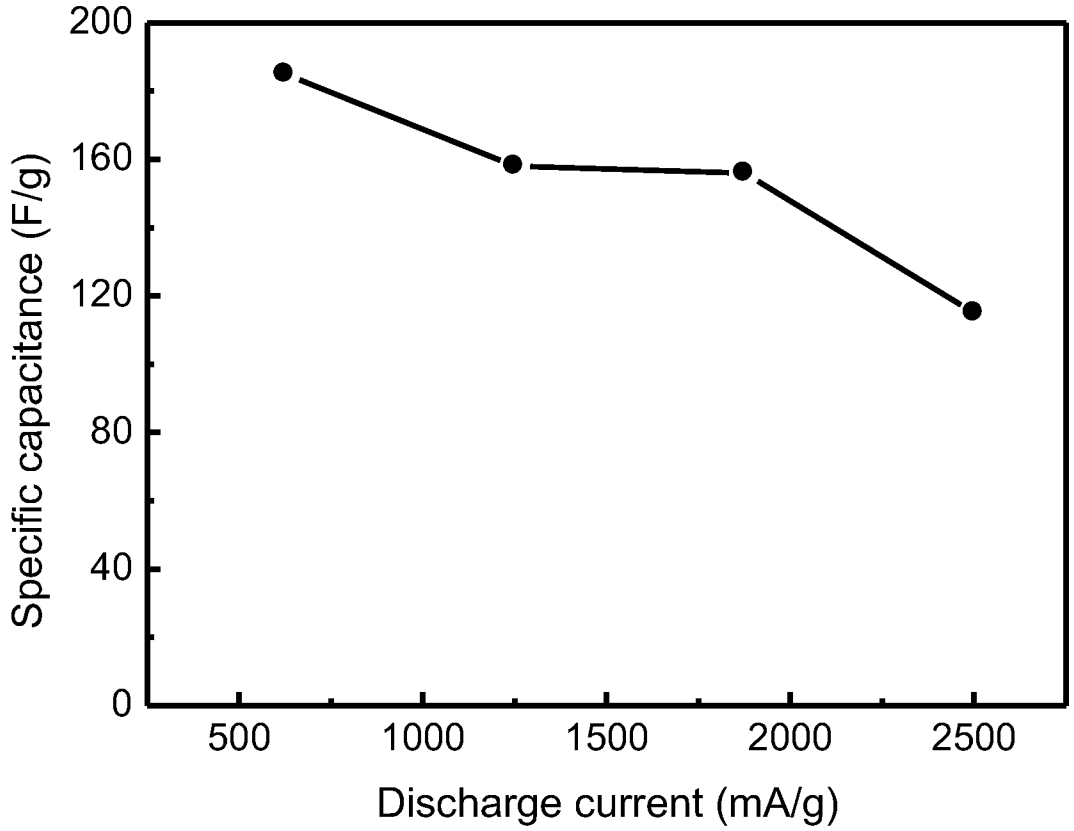
200
160
120
80
40
0
Specific capacitance (F/g)
500
1000
1500
2000
2500
Discharge current (mA/g)

FIG. 5

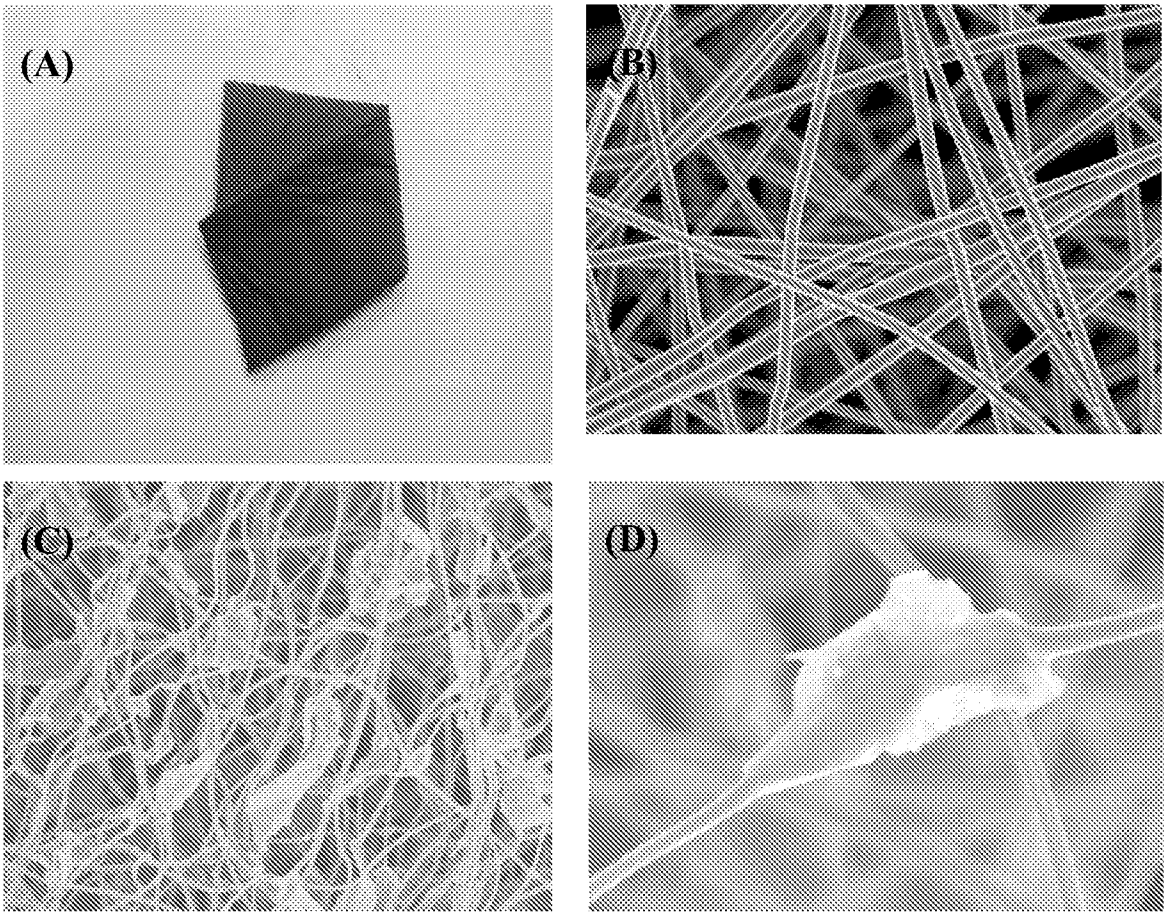

FIG. 6

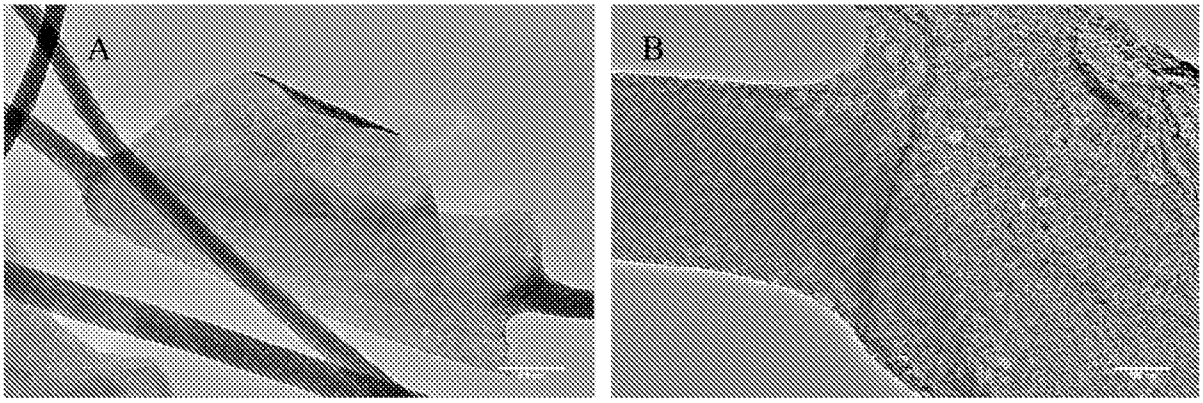

FIG. 7

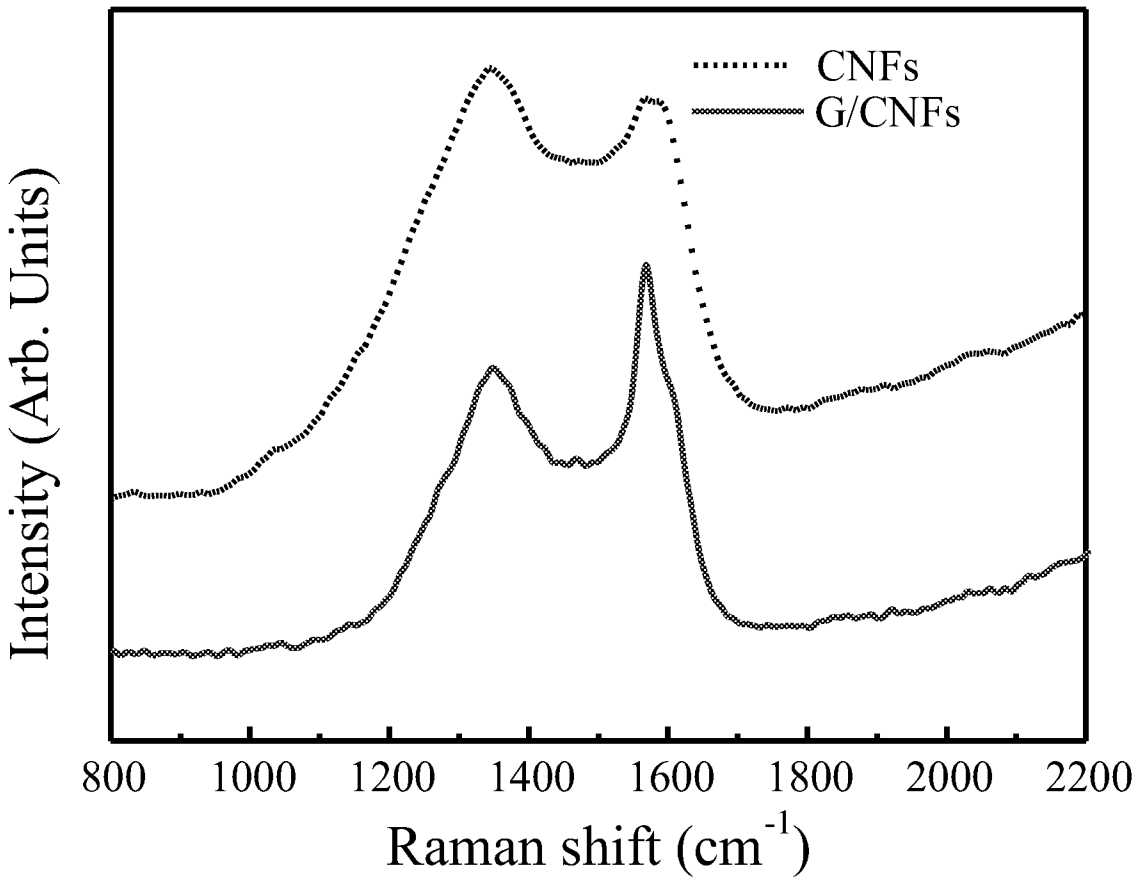
CNFs
G/CNFs
Intensity (Arb. Units)
800
1000
1200
1400
1600
1800
2000
2200
Raman shift (cm-1)

FIG. 8

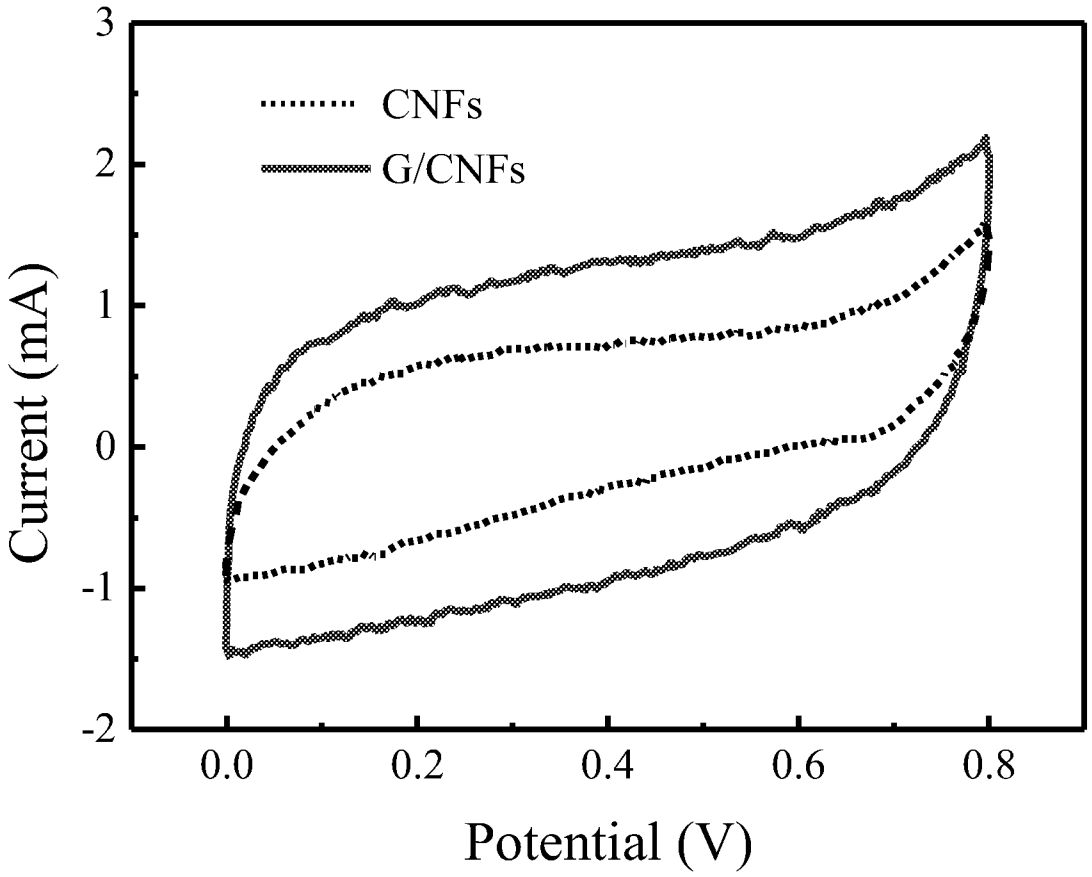

FIG. 9

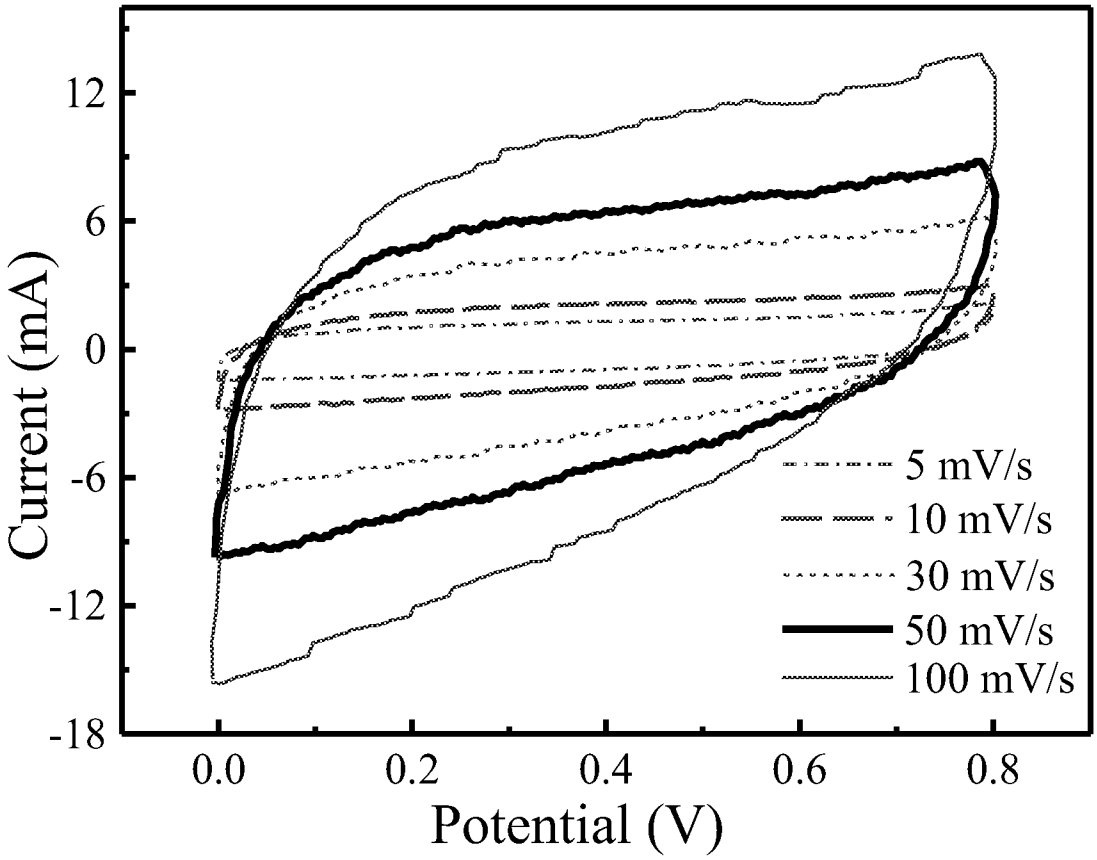
12
6
0
-6
-12
-18
Current (mA)
0.0
0.2
0.4
0.6
0.8
Potential (V)
5 mV/s
10 mV/s
30 mV/s
50 mV/s
100 mV/s

FIG. 10

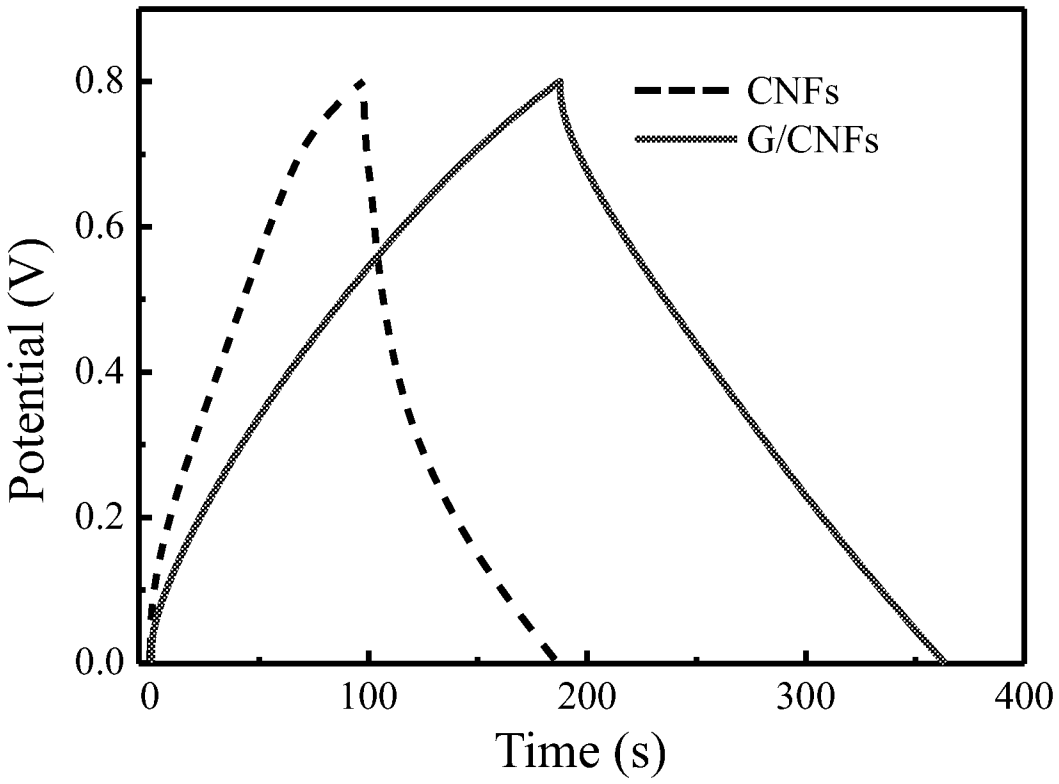

FIG. 11

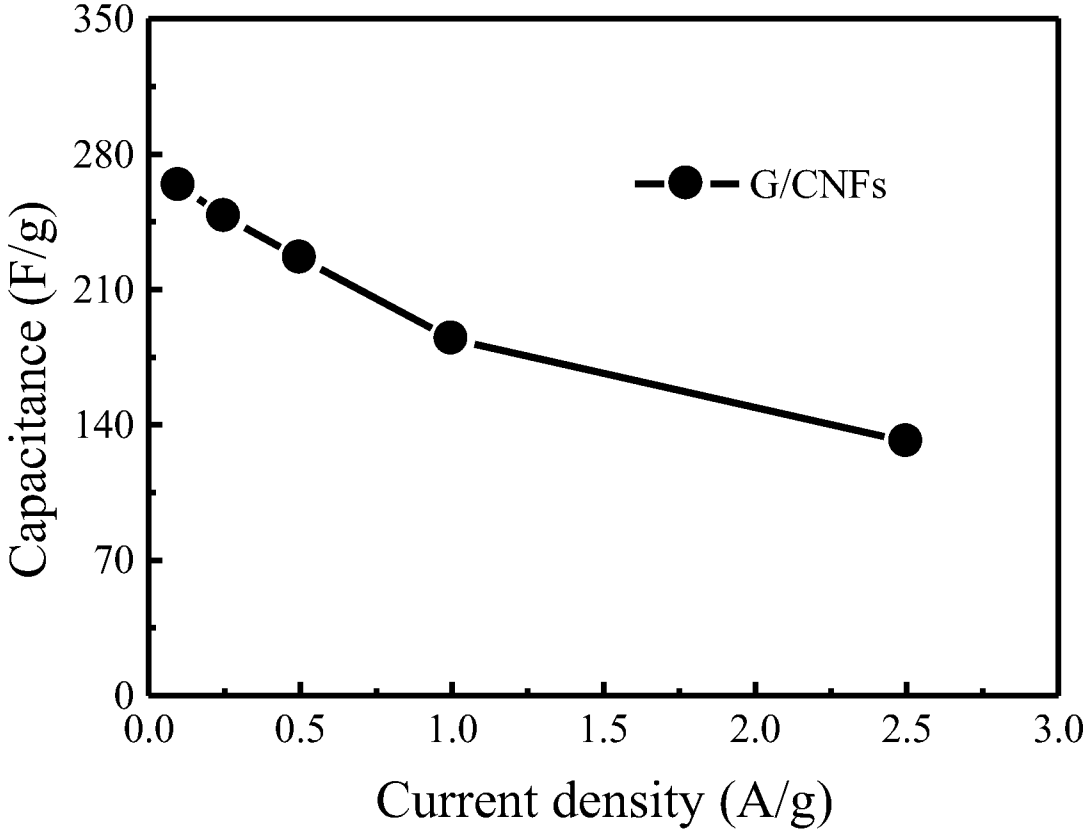
350
280
210
140
70
0
Capacitance (F/g)
G/CNFs
0.0
0.5
1.0
1.5
2.0
2.5
3.0
Current density (A/g)

FIG. 12

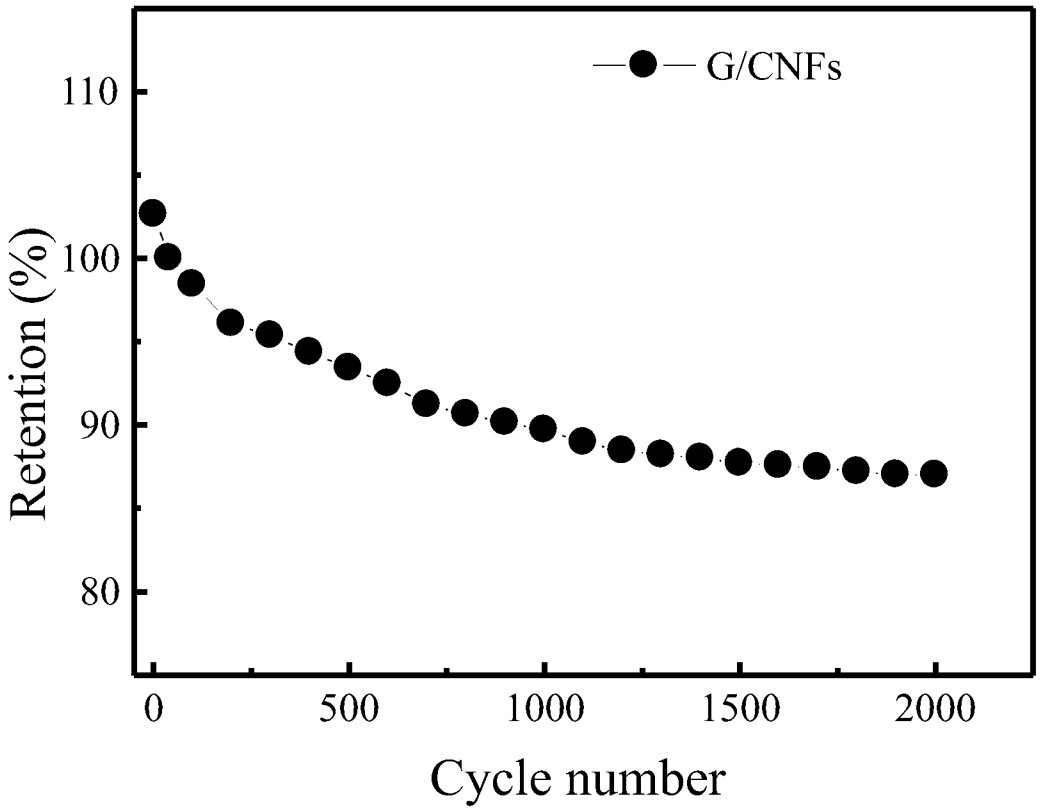
G/CNFs
110
100
90
80
Retention (%)
0
500
1000
1500
2000
Cycle number

FIG. 13

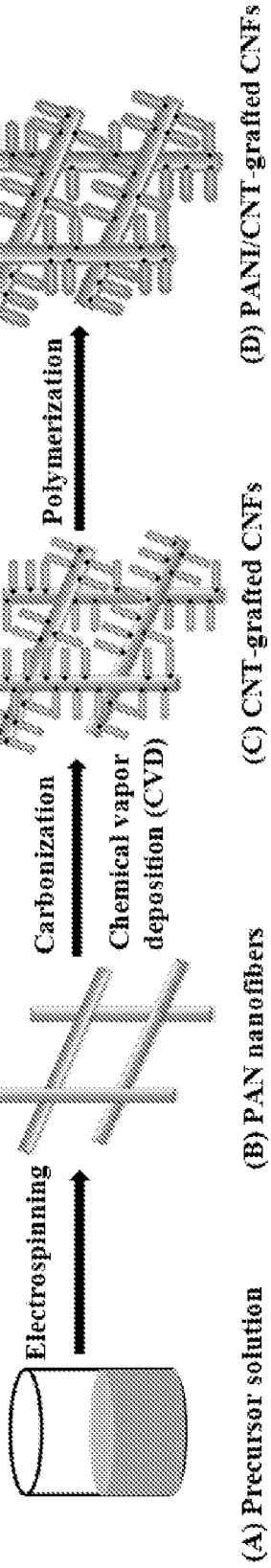
Electrospinning
Carbonization
Chemical vapor deposition (CVD)
Polymerization
(A) Precursor solution
(B) PAN nanofibers
(C) CNT-grafted CNFs
(D) PANI/CNT-grafted CNFs

FIG. 14

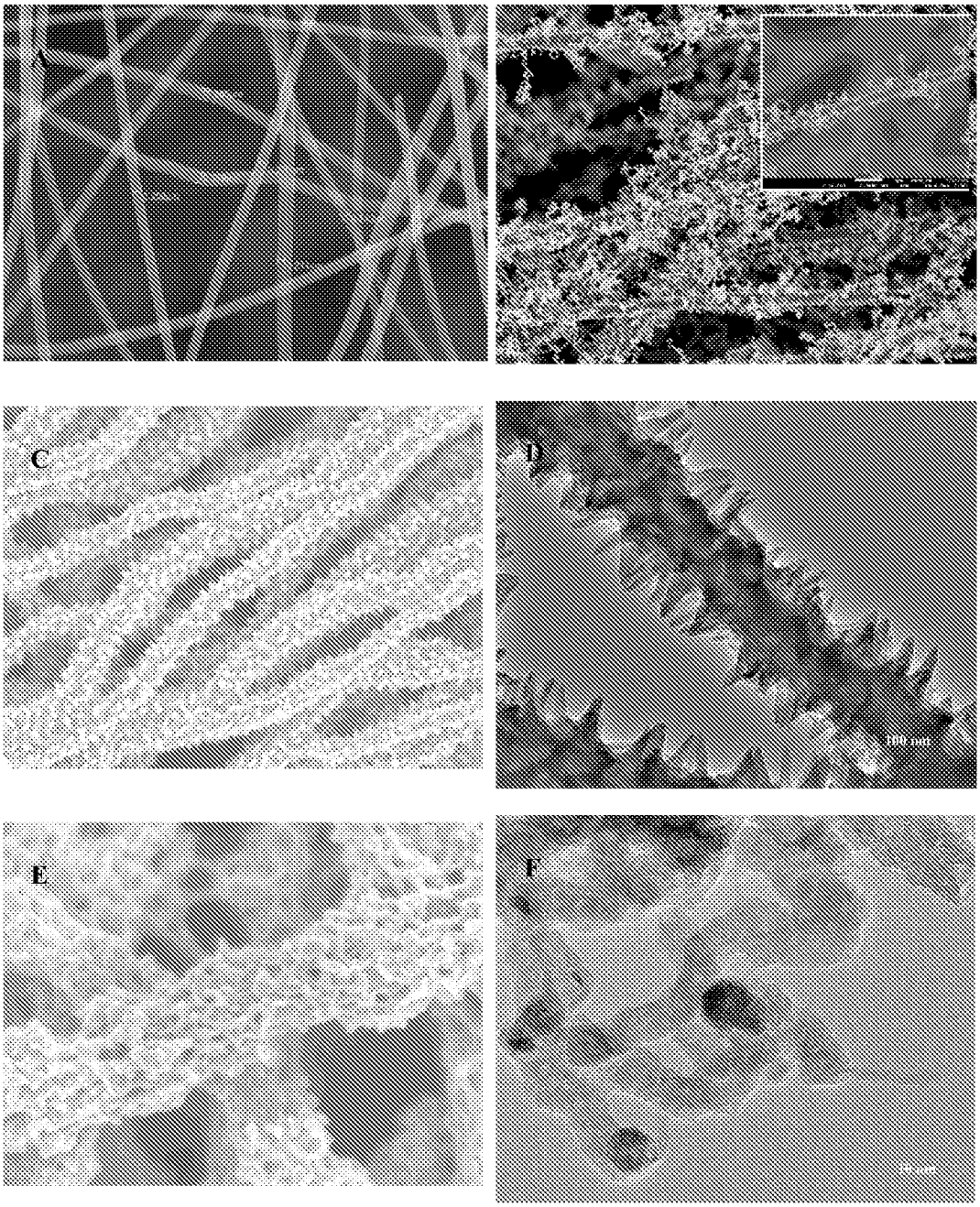

FIG. 15

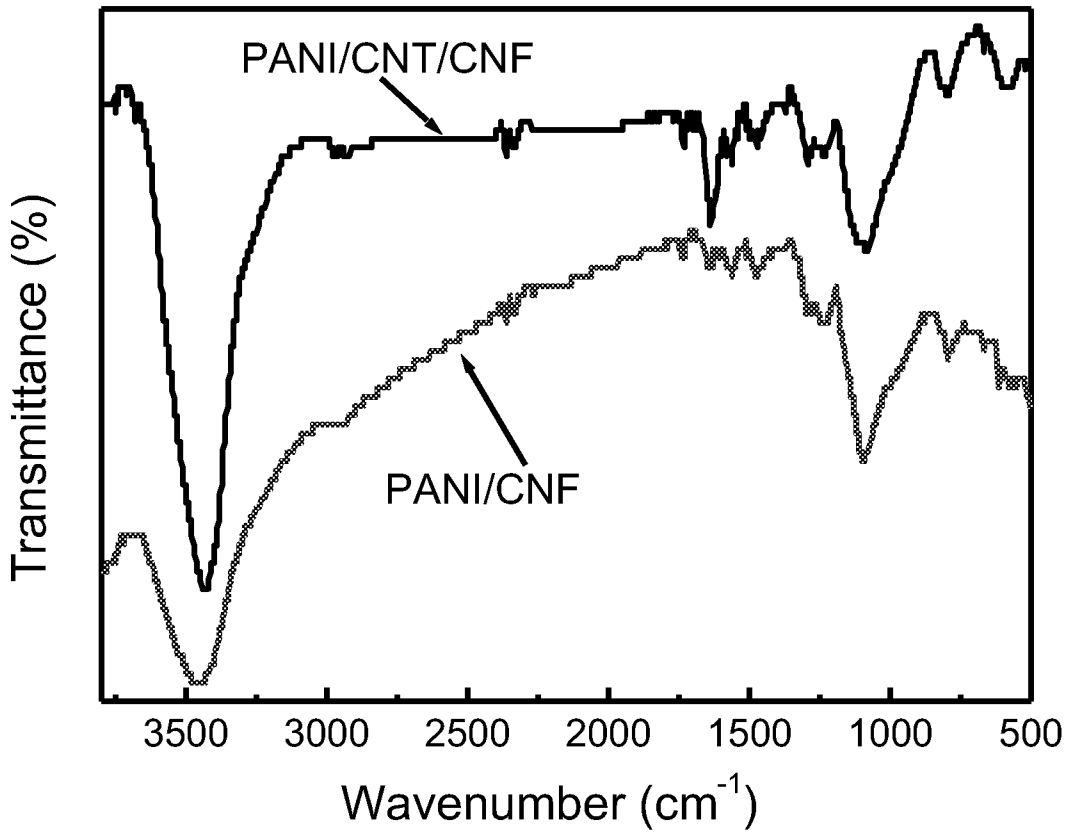
PANI/CNT/CNF
PANI/CNF
Transmittance (%)
3500
3000
2500
2000
1500
1000
500
Wavenumber (cm-1)

FIG. 16

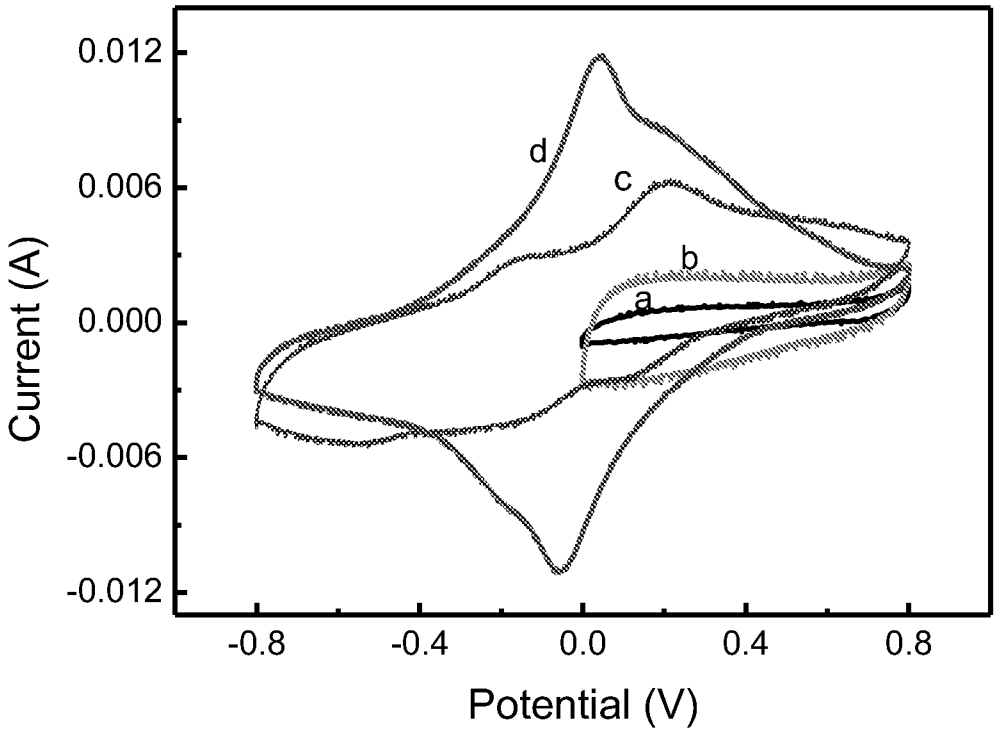

FIG. 17A

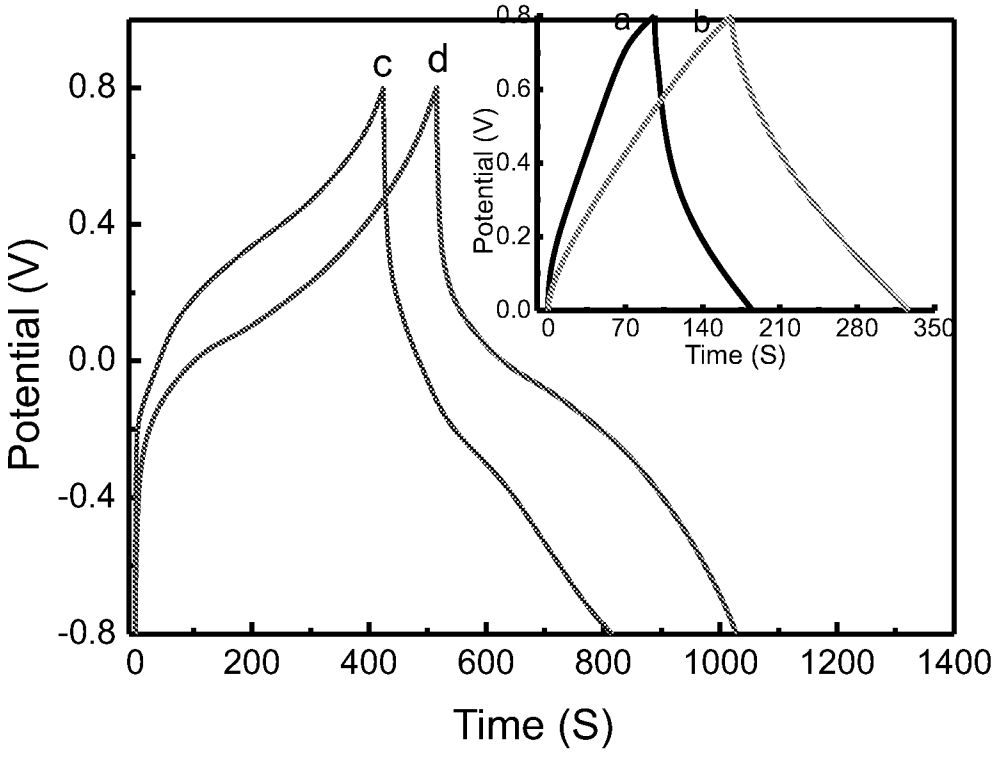

FIG. 17B

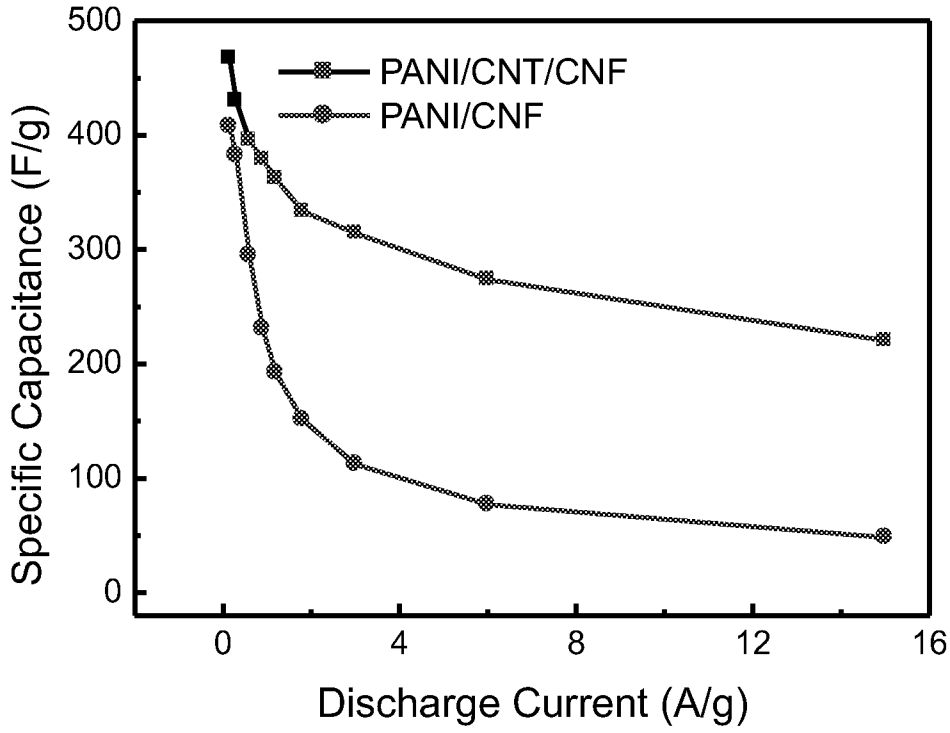

FIG. 18A

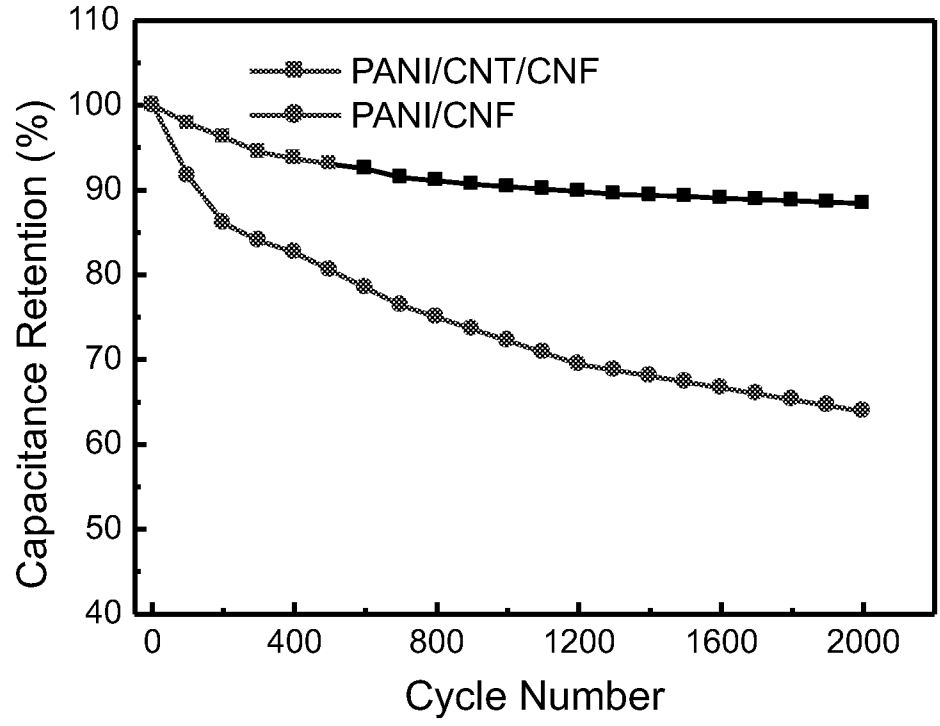

FIG. 18B

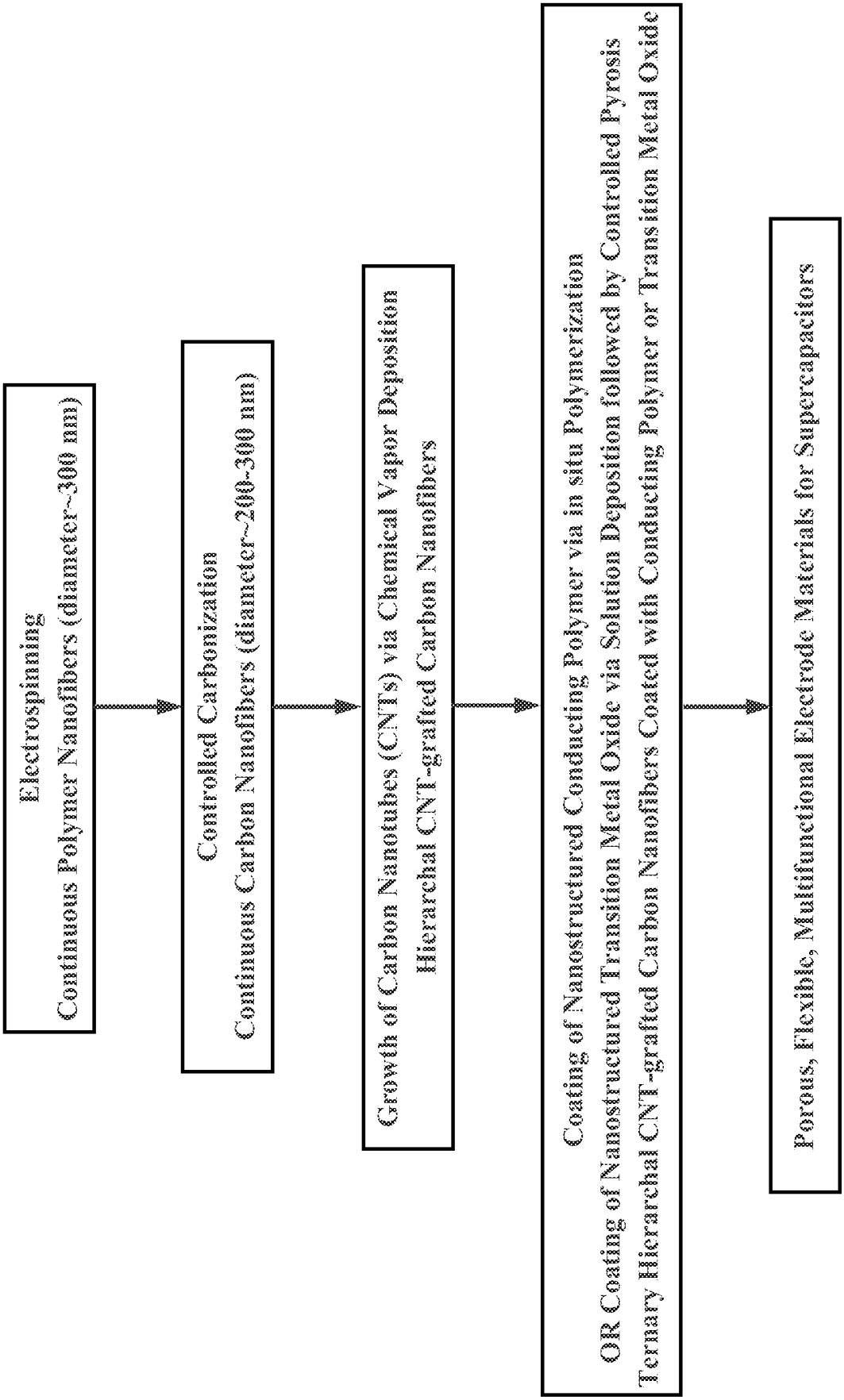
Electrospinning
Continuous Polymer Nanofibers (diameter~300 nm)
Controlled Carbonization
Continuous Carbon Nanofibers (diameter~200-300 nm)
Growth of Carbon Nanotubes (CNTs) via Chemical Vapor Deposition
Hierarchal CNT-grafted Carbon Nanofibers
Coating of Nanostructured Conducting Polymer via in situ Polymerization
OR Coating of Nanostructured Transition Metal Oxide via Solution Deposition followed by Controlled Pyrosis
Ternary Hierarchal CNT-grafted Carbon Nanofibers Coated with Conducting Polymer or Transition Metal Oxide
Porous, Flexible, Multifunctional Electrode Materials for Supercapacitors

FIG. 19

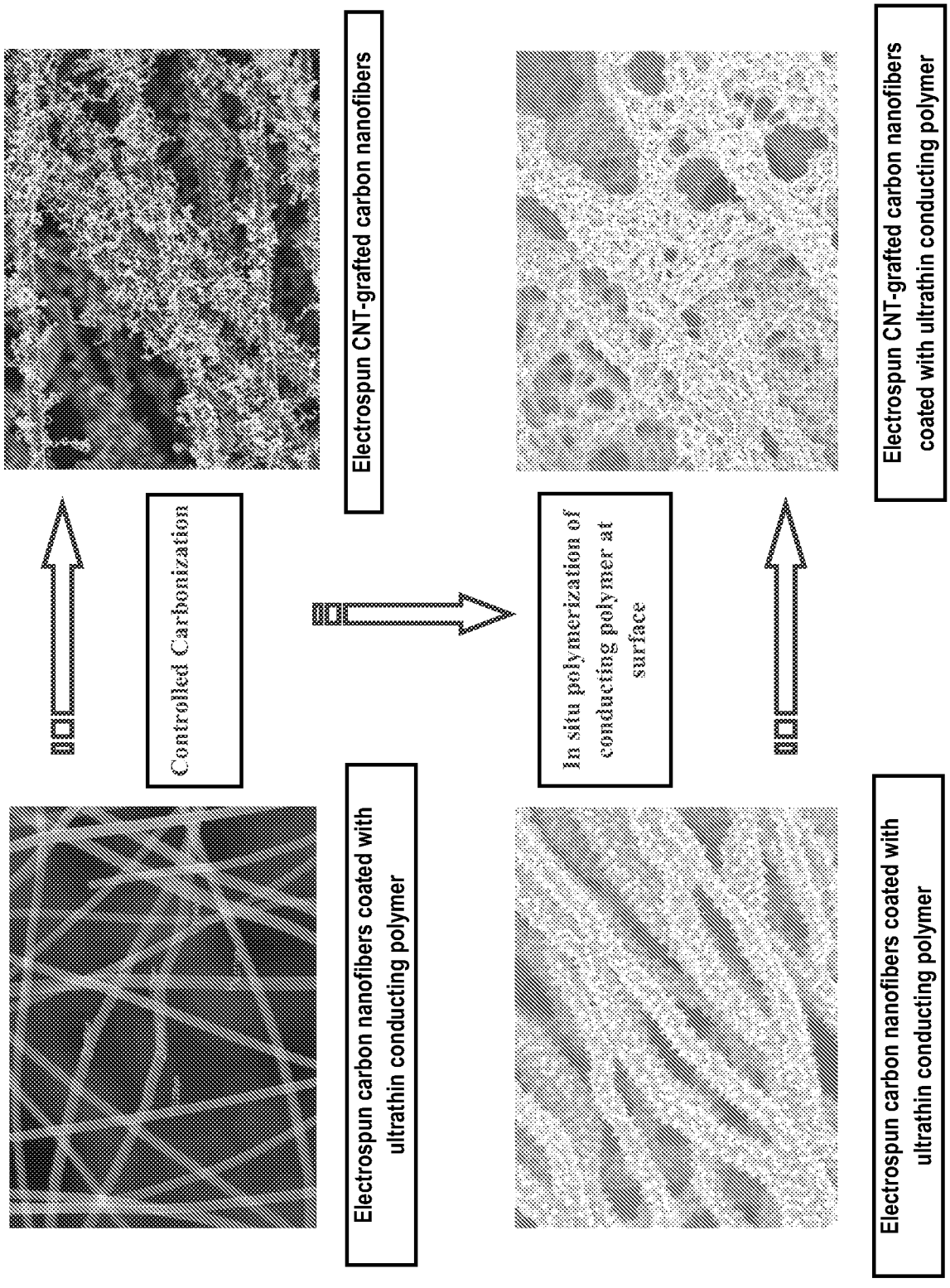
Electrospun carbon nanofibers coated with ultrathin conducting polymer
Controlled Carbonization
Electrospun CNT-grafted carbon nanofibers
In situ polymerization of conducting polymer at surface
Electrospun CNT-grafted carbon nanofibers coated with ultrathin conducting polymer
Electrospun carbon nanofibers coated with ultrathin conducting polymer

FIG. 20

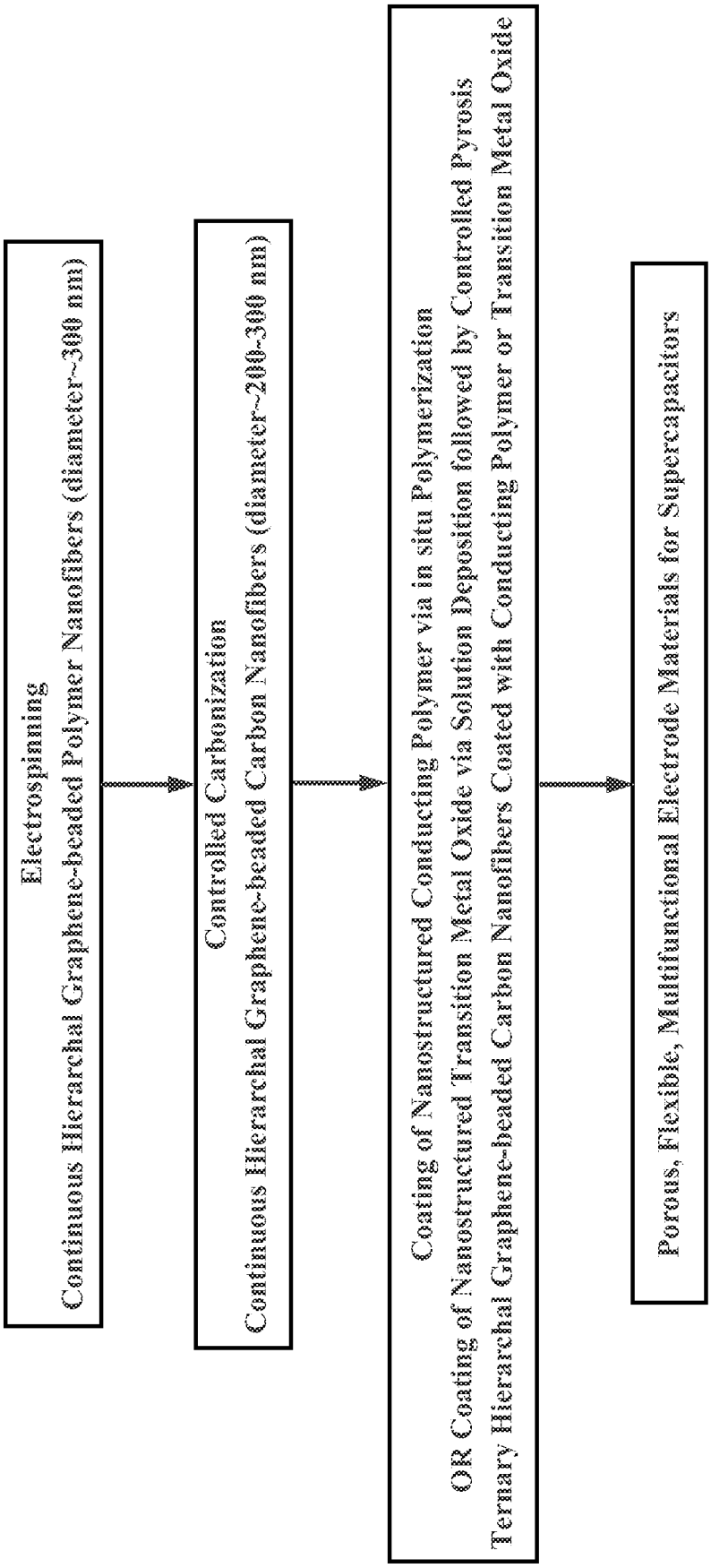
Electrospinning
Continuous Hierarchal Graphene-beaded Polymer Nanofibers (diameter~300 nm)
Controlled Carbonization
Continuous Hierarchal Graphene-beaded Carbon Nanofibers (diameter~200-300 nm)
Coating of Nanostructured Conducting Polymer via in situ Polymerization
OR Coating of Nanostructured Transition Metal Oxide via Solution Deposition followed by Controlled Pyrosis
Ternary Hierarchal Graphene-beaded Carbon Nanofibers Coated with Conducting Polymer or Transition Metal Oxide
Porous, Flexible, Multifunctional Electrode Materials for Supercapacitors

FIG. 21

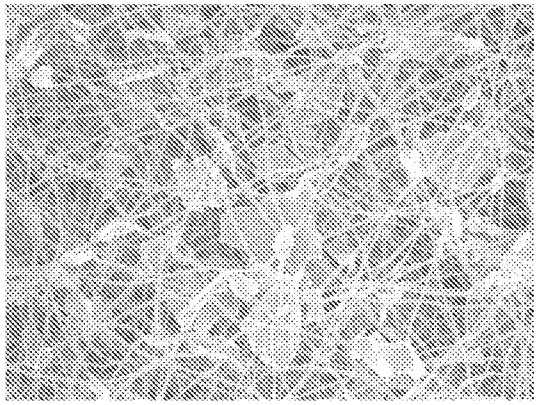

Electrospun graphene-beaded carbon nanofibers

In situ polymerization of conducting polymer at surface

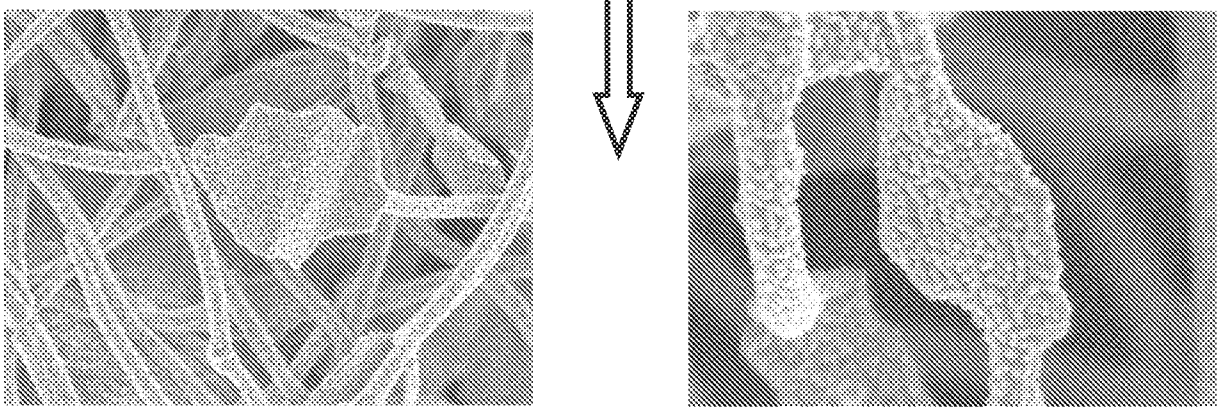

Electrospun graphene-beaded carbon nanofibers coated with ultrathin conducting polymer

FIG. 22

INTERNATIONAL SEARCH REPORT

PCT/US13/69906

A. CLASSIFICATION OF SUBJECT MATTER

IPC(8) - D01F 9/00; B29C 47/88; H01M 4/1393 (2014.01)

USPC - 428/367; 361/502; 977/742

According to International Patent Classification (IPC) or to both national classification and IPC

B. FIELDS SEARCHED

Minimum documentation searched (classification system followed by classification symbols)

IPC(8): D01F 9/00, 8/00; B29C 47/88, 47/00; H01M 4/1393; H01G 11/00; B32B 5/02; B01J 31/06 (2014.01)
USPC: 428/367, 373, 401; 264/465, 434; 429/532; 361/502; 977/742, 762

Documentation searched other than minimum documentation to the extent that such documents are included in the fields searched

Electronic data base consulted during the international search (name of data base and, where practicable, search terms used)

MicroPatent (US-G, US-A, EP-A, EP-B, WO, JP-bib, DE-C,B, DE-A, DE-T, DE-U, GB-A, FR-A); ProQuest; Google Scholar; IP.com; carbon, nanotube, CNT, nanofiber, CNF, precursor solution, polymer, polyaniline, coating, grow, deposit, metal oxide

C. DOCUMENTS CONSIDERED TO BE RELEVANT

Category*	Citation of document, with indication, where appropriate, of the relevant passages	Relevant to claim No.
X --- Y	US 2009/0068461 A1 (RENEKER, DH et al.) 12 March 2009; paragraphs [0036]-[0039], [0050]-[0057], [0080], [0090]-[0091], [0099], [0101], [0104]-[0106]; claims 15, 17	1-4, 8-11, 13 --- 5-7, 12, 14-20
Y	YAN, J et al. Preparation of graphene nanosheet/carbon nanotube/polyaniline composite as electrode material for supercapacitors. Journal of Power Sources, Elsevier, Vol. 195, No. 9, 01 May 2010, pp. 3041-3045 [online], [retrieved on 2014-02-19]. Retrieved from the Internet <URL: http://www.sciencedirect.com/science/article/pii/S0378775309020369> <DOI: 10.1016/j.jpowsour.2009.11.028>; abstract; page 3041, column 1, paragraph 1, column 2, paragraph 2, page 3043, column 1, paragraph 3	5-7, 12, 14-20
Y	US 2008/0280058 A1 (KRUNKS, M et al.) 13 November 2008; abstract; paragraphs [0003], [0015]	7, 19

☐ Further documents are listed in the continuation of Box C. ☐

* Special categories of cited documents:

"A" document defining the general state of the art which is not considered to be of particular relevance

"E" earlier application or patent but published on or after the international filing date

"L" document which may throw doubts on priority claim(s) or which is cited to establish the publication date of another citation or other special reason (as specified)

"O" document referring to an oral disclosure, use, exhibition or other means

"P" document published prior to the international filing date but later than the priority date claimed

"T" later document published after the international filing date or priority date and not in conflict with the application but cited to understand the principle or theory underlying the invention

"X" document of particular relevance; the claimed invention cannot be considered novel or cannot be considered to involve an inventive step when the document is taken alone

"Y" document of particular relevance; the claimed invention cannot be considered to involve an inventive step when the document is combined with one or more other such documents, such combination being obvious to a person skilled in the art

"&" document member of the same patent family

Date of the actual completion of the international search	Date of mailing of the international search report
21 February 2014 (21.02.2014)	07 MAR 2014
Name and mailing address of the ISA/US Mail Stop PCT, Attn: ISA/US, Commissioner for Patents P.O. Box 1450, Alexandria, Virginia 22313-1450 Facsimile No. 571-273-3201	Authorized officer: Shane Thomas PCT Helpdesk: 571-272-4300 PCT OSP: 571-272-7774